DYNATECH CORPORATION

FREE VIBRATIONS OF THE PRESTRESSED TOROIDAL MEMBRANE

Report No. 474

Prepared by:

Atis A. Liepins

Submitted to:

National Aeronautics and Space Administration
Washington, D. C.

(Prepared under Contracts NASw-600 and NASw-881)

May 22, 1964

Progress through Research

DYNATECH

FREE VIBRATIONS OF THE PRESTRESSED TOROIDAL MEMBRANE

Report No. 474

Prepared by:

Atis A. Liepins

Submitted to:

National Aeronautics and Space Administration
Washington, D. C.

(Prepared under Contracts NASw-600 and NASw-881)

May 22, 1964

DYNATECH CORPORATION
17 Tudor Street
Cambridge, Massachusetts 02139

Progress through Research

TABLE OF CONTENTS

DYNATECH

FREE VIBRATIONS OF THE PRESTRESSED TOROIDAL MEMBRANE

By Atis A. Liepins

SUMMARY

A numerical analysis of the free vibrations of the prestressed circular toroidal membrane is presented. Frequency curves and mode shapes are displayed and compared with those of the prestressed circular string and those obtained from classical ring theory. The effect of prestress on frequencies is shown.

INTRODUCTION

We are concerned with the natural frequencies and modes of vibration of a prestressed toroidal membrane. Prestress caused by internal pressure and centrifugal forces is considered. The torus is supported in a free - free manner.

The purpose of this investigation is to demonstrate a numerical procedure and to show the nature of the natural frequencies and modes of vibration by numerical results.

SYMBOLS

a_n, b_n	Fourier coefficients of string modes
g	acceleration of gravity
h	thickness of membrane and string
k	$(1 - \nu^2)\kappa$
k*	$(1 + \nu^2)\kappa$
p	pressure
r	$(1 - \epsilon \cos \alpha)/\epsilon$
u	Fourier coefficient of meridional displacement
$\bar{u}$	meridional displacement (Figure 1)
v	Fourier coefficient of circumferential displacement
$\bar{v}$	circumferential displacement (Figure 1)

w	Fourier coefficient of normal displacement
$\bar{w}$	normal displacement (Figure 1)
A_1, A_2, A_3 B_1, B_2, B_3	coefficients defined in Appendix A
C, M, N, Q, S $T_1\ T_2\ \ldots\ T_6$	functions defined in Appendix A
E	Young's modulus
$E_\alpha, E_\theta, E_{\alpha\theta}$	membrane strains
$F_1 \ldots F_4$	junctions of distortions
$N_\alpha, N_\theta, N_{\alpha\theta}$	membrane forces per unit length
N_s	String force
R	radius of generating circle of the torus (Figure 1); radius of string
S_α, S_θ	membrane prestress forces
S_s	string prestress force
U	circumferential displacement of string
W	normal displacement of string
α	position angle (Figure 1)
ϵ	ratio of the two radii of the torus (Figure 1)
θ	circumferential angle (Figure 1)
κ	pR/Eh, prestress parameter
λ	$\left(\rho R^2/E\epsilon^2\right)\ \omega^2$, frequency parameter

ν	Poisson's ratio
ρ	material density
ϕ	Fourier coefficient of ϕ_α
ϕ_α, ϕ_θ, $\phi_{\alpha\theta}$	membrane rotations
ϕ_s	string rotation
ω	circular frequency
Γ	$\rho h(\Omega R)^2 / pR\epsilon^2$
Δ	spacing between stations
Ω	speed of rotation of membrane

Matrices

A, B, C, D, E, F, G	3 x 3 matrices
$\overline{A}$, $\overline{B}$, $\overline{C}$	2 x 2 matrices
Z	1 x 3 column matrix
$\overline{Z}$	1 x 2 column matrix

Indices

i	station
I	last station
m	Fourier index of string vibrations
n	Fourier index of membrane vibrations

FUNDAMENTAL EQUATIONS

Equations suitable for the analysis of vibrations of prestressed membranes have been recently derived by Budiansky (Ref. 1). For the circular torus these are (refer to Figure 1):

Equilibrium

$$\frac{\partial}{\partial\alpha}(rN_\alpha) + \frac{\partial N_{\alpha\theta}}{\partial\theta} - N_\theta \sin\alpha + rS_\alpha\left(\frac{\partial E_\alpha}{\partial\alpha} - \phi_\alpha\right)$$

$$+ S_\theta\left[\frac{\partial}{\partial_{\alpha\theta}}\left(E_{\alpha\theta} - \phi_{\alpha\theta}\right) + \left(E_\alpha - E_\theta\right)\sin\alpha\right] + pRr\phi_\alpha + \rho hR\omega^2 r\bar{u} = 0 \tag{1}$$

$$\frac{\partial N_\theta}{\partial\theta} + \frac{\partial}{\partial\alpha}\left(rN_{\alpha\theta}\right) + N_{\alpha\theta}\sin\alpha + rS_\alpha\frac{\partial}{\partial\alpha}\left(E_{\alpha\theta} + \phi_{\alpha\theta}\right)$$

$$+ S_\theta\left[\frac{\partial E_\theta}{\partial\theta} + 2E_{\alpha\theta}\sin\alpha + \phi_\theta\cos\alpha\right] + pRr\phi_\theta + \rho hR\omega^2 r\bar{v} = 0 \tag{2}$$

$$rN_\alpha - N_\theta\cos\alpha + rS_\alpha\left(\frac{\partial\phi_\alpha}{\partial\alpha} + E_\alpha\right)$$

$$+ S_\theta\left[\frac{\partial\phi_\theta}{\partial\theta} + \phi_\alpha\sin\alpha - E_\theta\cos\alpha\right] + pRr\left(E_\alpha + E_\theta\right) - \rho hR\omega^2 r\bar{w} = 0 \tag{3}$$

Strain Displacement

$$RE_\alpha = \frac{\partial\bar{u}}{\partial\alpha} + \bar{w} \tag{4}$$

$$rRE_\theta = \frac{\partial\bar{v}}{\partial\theta} + \bar{u}\sin\alpha - \bar{w}\cos\alpha \tag{5}$$

$$2rRE_{\alpha\theta} = r\frac{\partial\bar{v}}{\partial\alpha} + \frac{\partial\bar{u}}{\partial\theta} - \bar{v}\sin\alpha \tag{6}$$

$$R\phi_\alpha = -\frac{\partial \bar{w}}{\partial \alpha} + \bar{u} \tag{7}$$

$$-rR\phi_\theta = \frac{\partial \bar{w}}{\partial \theta} + \bar{v}\cos\alpha \tag{8}$$

$$-2rR\phi_{\alpha\theta} = \frac{\partial \bar{u}}{\partial \theta} - \frac{\partial}{\partial \alpha}(r\bar{v}) \tag{9}$$

Constitutive Relations

$$Eh\,E_\alpha = N_\alpha - \nu N_\theta \tag{10}$$

$$Eh\,E_\theta = N_\theta - \nu N_\alpha \tag{11}$$

$$Eh\,E_{\alpha\theta} = (1+\nu)\,N_{\alpha\theta} \tag{12}$$

The above constitute 12 equations for the 12 unknowns N_α, N_θ, $N_{\alpha\theta}$, E_α, E_θ, $E_{\alpha\theta}$, ϕ_α, ϕ_θ, $\phi_{\alpha\theta}$, $\bar{u}$, $\bar{v}$, and $\bar{w}$. S_α and S_θ describe the state of prestress. They are determined from a separate analysis of the torus subjected to static internal pressure and centrifugal loads. An analysis based on the linear membrane theory (Ref. 2) gives

$$S_\alpha = pR\,\frac{1 - \frac{1}{2}\epsilon\cos\alpha}{1 - \epsilon\cos\alpha} \tag{13}$$

$$S_\theta = \frac{1}{2}pR + \rho h\,(\Omega Rr)^2$$

Analyses of the torus under internal pressure based upon nonlinear theories (Ref. 3 and 4) show that the linear meridional stress, S_θ, can be in error by 18%. The significant difference, however, between the linear and nonlinear stress distributions is confined to a small area of the torus. The error in the circumferential stress is negligible. Furthermore, the stresses according to the nonlinear theory depend on deformations. Such deformations are assumed to be negligible in the derivation of the fundamental equations (1 - 12). Hence, it is assumed that the state of prestress determined according to the linear membrane theory is adequately accurate for the analysis of the free vibrations.

When the prestress is given by Equation 13, the solutions of the fundamental equations (1 - 12) are such that either w and v are even, u is odd or w and v are odd, and u is an even function of α with respect to $\alpha = 0$ and $\alpha = \pi$. These two groups of solutions will be called symmetric and antisymmetric modes, respectively.

REDUCTION TO ORDINARY SECOND ORDER DIFFERENTIAL EQUATIONS

The fundamental equations (1 - 12) can be reduced in the usual manner to three differential equations in $\bar{u}$, $\bar{v}$, and $\bar{w}$. However, to obtain a rapid convergence of the finite difference scheme, described in the following section, we obtain three equations in u, v, and ϕ as follows. First, expand $\bar{u}$, $\bar{v}$, $\bar{w}$, and ϕ_α in Fourier series

$$\bar{u} = R \sum_{n=0}^{\infty} u_n(\alpha) \cos n\theta$$

$$\bar{v} = R \sum_{n=0}^{\infty} v_n(\alpha) \sin n\theta$$

$$\bar{w} = R \sum_{n=0}^{\infty} w_n(\alpha) \cos n\theta$$

$$\phi_\alpha = \sum_{n=0}^{\infty} \phi_n(\alpha) \cos n\theta \qquad (14)$$

Next, substitute Equations (4 - 6) and (8 - 14) into Equations (1 - 3). The resultant equations together with Equation (7) constitute four ordinary differential equations in u_n, v_n, w_n, and ϕ_n. They are of the form

$$F_1(u'', u', u, v', v, w', w, \phi) = 0 \qquad (15)$$

$$F_2(u', u, v'', v', v, w) = 0 \qquad (16)$$

$$F_3(u', u, v, w, \phi', \phi) = 0 \qquad (17)$$

$$\phi + w' - u = 0 \qquad (18)$$

In the above and all subsequent equations, the subscript n on the Fourier coefficients has been dropped. Primes indicate differentiation with respect to α.

Equation (17) can be solved for w in terms of u, v, and ϕ:

$$Qw = T_1 u' + T_2 u + T_3 v + \kappa \left(1 + \frac{1}{2}C\right) \phi' + \frac{1}{2}\kappa \, MS\phi \qquad (19)$$

and the first derivative of w can be expressed as

$$Qw' = -Q'w + F_4 (u'', u', u, v', v, \phi'', \phi', \phi) \qquad (20)$$

All coefficients in Equations (19 and 20) are defined in Appendix A.

Now, multiply Equation (15) by Q and eliminate Qw' using Equation (20). Then multiply the resultant equation by Q and eliminate Qw using Equation (19). In the same way eliminate w' from Equation (18). Finally, multiply Equation (16) by Q and eliminate Qw. The resultant three differential equations for u, v, and ϕ are each of the second order. They can be written in matrix form

$$AZ'' + BZ' + CZ = 0 \qquad (21)$$

where

$$Z = \begin{Bmatrix} u \\ v \\ \phi \end{Bmatrix}$$

The elements of A, B, and C are defined in Appendix A.

The basic Equations (21) simplify for several special classes of vibrations. In the case of axisymmetric vibrations, n = 0, v = 0, and the second equation of Equations (21) (equilibrium in θ direction) is satisfied identically. Then, Equations (21) becomes

$$\bar{A}\bar{Z}'' + \bar{B}\bar{Z}' + \bar{C}\bar{Z} = 0 \qquad (22)$$

where

$$\bar{Z} = \begin{Bmatrix} u \\ \phi \end{Bmatrix}$$

The elements of $\bar{A}$, $\bar{B}$, and $\bar{C}$ are the remaining elements of A, B, and C if the second row and column are deleted.

Furthermore, if the torus is not prestressed ($\kappa = 0$), ϕ can be eliminated from Equations (22). The resultant differential equation for u is:

$$\left[\lambda - \left(\frac{\cos\alpha}{1 - \epsilon\cos\alpha}\right)^2\right] A_1 u'' + A_2 u' + A_3 u = 0 \qquad (23)$$

where A_1, A_2, and A_3 are given in Appendix A.

In the case of circumferential vibrations, $u = w = \phi = 0$, $n = 0$, $\bar{v} = v(\alpha)$, and the first and third equations of Equation (21) are satisfied identically. The governing differential equation for v is

$$B_1 v'' + B_1 v' + B_3 v = 0 \tag{24}$$

The coefficients are given in Appendix A.

NUMERICAL ANALYSIS

The geometry and prestress are symmetrical about $\alpha = 0$ and $\alpha = \pi$. Hence, we need to consider only one-half of the torus corresponding to the range $0 \leq \alpha \leq \pi$. Let this range be subdivided by I + 1 equally spaced stations. Then the spacing between stations is

$$\Delta = \pi/I$$

and the position angle for the i^{th} station is

$$\alpha_i = i\Delta \qquad i = 0, 1, 2, \ldots . I$$

The differential Equations (21) at the i^{th} station can then be written

$$A_i Z_i'' + B_i Z_i' + C_i Z_i = 0 \qquad i = 0, 1, 2, \ldots . I \tag{25}$$

The elements of A_i, B_i, and C_i are those of A, B, and C with α replaced by $i\Delta$.

The derivatives of z at the i^{th} station are approximated by the central difference formulas

$$Z_i' = \frac{1}{2\Delta} (Z_{i+1} - Z_{i-1})$$

$$Z_i'' = \frac{1}{\Delta^2} (Z_{i+1} - 2Z_i + Z_{i-1}) \tag{26}$$

With these formulas we obtain from Equation (25) the set of finite difference equations

$$D_i Z_{i+1} + E_i Z_i + F_i Z_{i-1} = 0 \qquad i = 0, 1, 2, \ldots . I \tag{27}$$

where

$$D_i = \frac{2}{\Delta} A_i + B_i$$

$$E_i = -\frac{4}{\Delta} A_i + 2\Delta C_i$$

$$F_i = \frac{2}{\Delta} A_i - B_i \qquad (28)$$

The difference Equations (27) are augmented by conditions at i = 0 and i = I. These end conditions are obtained from considerations of continuity of the displacement functions u, v, and w. They are

$$Z_{-1} = \pm G Z_1$$

$$Z_{I+1} = \pm G Z_{I-1}$$

where

$$G = \begin{bmatrix} -1 & & \\ & 1 & \\ & & -1 \end{bmatrix} \qquad (29)$$

Plus and minus signs refer to symmetric and antisymmetric modes respectively.

The eigenvalues of the set of difference Equations (27) are obtained by trial and error. Inthis procedure a Gaussian elimination technique is employed, applicable to equations with a tridiagonal matrix (Ref. 5). The equations for this procedure are obtained as follows. Let

$$Z_i = -P_i Z_i + 1 \qquad (30)$$

Substitution of the above expression into Equations (27) gives the recurrence relation

$$P_i = \left[E_i - F_i P_{i-1}\right]^{-1} D_i \quad i = 1, 2, 3, \ldots\ldots I-1 \qquad (31)$$

Now, write the difference Equations (27) at i = 0 and eliminate Z_{-1} using Equations (29). The result is

$$E_0 Z_0 + \left[D_0 \pm F_0 G\right] Z_1 = 0$$

which provides the expression

$$P_0 = E_0^{-1} \left[D_0 \pm F_0 G\right] \qquad (32)$$

Equation (32) together with the recurrence relation Equation (31) provides all the P's up to P_{I-1}. Finally, write the difference Equations (27) at i = I. Eliminate Z_{I+1} using Equations (29), and Z_{I-1} using Equation (30). The result is

$$\left[E_I - \left[F_I \pm D_I G\right] P_{I-1} Z_I\right] = 0 \qquad (33)$$

Since $Z_I \neq 0$, we must require that the determinant

$$\nabla = \left| E_I - \left[F_I \pm D_I G \right] P_{I-1} \right| \tag{34}$$

vanish. Equation (34) is effectively a frequency equation. A value of λ which gives $\nabla = 0$ is a natural frequency of vibration.

The mode shape corresponding to a natural frequency can be calculated, once a λ for which $\nabla = 0$ and the corresponding P matrices are obtained. We set the amplitude of one of the displacements at i = I equal to unity and calculate the remaining displacements at i = I from two of the Equations (33). Thus, for the symmetric modes

$$Z_I = \begin{Bmatrix} 0 \\ 1 \\ 0 \end{Bmatrix} \tag{35}$$

For antisymmetric modes

$$Z_I = \begin{Bmatrix} 1 \\ 0 \\ \phi_I \end{Bmatrix} \tag{36}$$

where

$$\phi_I = - \frac{E_{31(I)} - \left(D_{31(I)} + F_{31(I)} \right) P_{11(I-1)} + \left(D_{32(I)} - F_{32(I)} \right) P_{21(I-1)} - \left(D_{33(I)} + F_{33(I)} \right) P_{31(I-1)}}{E_{33(I)} - \left(D_{31(I)} + F_{31(I)} \right) P_{13(I-1)} + \left(D_{32(I)} - F_{32(I)} \right) P_{23(I-1)} - \left(D_{33(I)} + F_{33(I)} \right) P_{33(I-1)}} \tag{37}$$

The remaining Z's can then be calculated from Equations (30).

The w displacement is obtained from Equation (19). In finite difference form the equation reads

$$w_i = \frac{1}{Q_i} \left[\frac{1}{2\Delta} T_{1(i)} \left(u_{i+1} - u_{i-1} \right) + T_{2(i)} u_i + T_{3(i)} v_i + \frac{\kappa}{2\Delta} \left(1 + \frac{1}{2} C_i \right) \left(\phi_{i+1} - \phi_{i-1} \right) + \frac{\kappa}{2} M_i S_i \phi_i \right]$$

$$i = 1, 2, 3 \ldots\ldots I-1$$

$$w_o = \frac{1}{Q_o} \left[\frac{1}{\Delta} T_{1(o)} u_1 + T_{3(o)} v_o + \frac{\kappa}{\Delta} \left(1 + \frac{1}{2} C_o \right) \phi_1 \right]$$

$$w_I = \frac{1}{Q_I} \left[-\frac{1}{\Delta} T_{1(I)} u_{I-1} + T_{3(I)} v_I - \frac{\kappa}{\Delta} \left(1 + \frac{1}{2} C_I \right) \phi_{I-1} \right] \tag{38}$$

The computation procedure is summarized as follows:

1. Assume a value of λ;
2. With the assumed λ, calculate the elements of the A, B, and C matrices at all stations from equations given in Appendix A;
3. Calculate the matrices D_i, E_i, F_i, and P_i from Equations (28), (31), and (32);
4. Evaluate the determinant ∇, Equation (34);
5. Repeat steps 1 - 4 to obtain a plot of ∇ versus λ. A typical plot is shown in Figure 2.
6. Calculate the mode shape corresponding to a natural frequency from Equations (30)and (35 - 38).

The equations in this procedure were programmed for the digital computer.

The numerical analysis of Equations (22 - 24) is similar to that described above for Equation (21). The equations of these analysis were also programmed for the digital computer.

RESULTS AND DISCUSSION

Natural frequencies and mode shapes for n = 0, 1, 2, 3 and circumferential vibrations are computed. Prestress due to internal pressure with intensities corresponding to $\kappa = 0.002$, 0.0001, and 0 is considered. The effect of centrifugal forces is determined for two specific geometries.

The frequencies and mode shapes of two limiting cases are of interest in the interpretation of the results:

1. The hollow ring (classical thin ring theory, Reference 6).
2. The prestressed circular string.

The "ring" frequencies and mode shapes are approximations to the overall deformation of the torus when ϵ is small. They are shown in Figure 3. The "string" frequencies and mode shapes are associated with distortions of the cross section. There are two families of "string" modes with the following frequencies:

$$\text{Lower family:} \quad \lambda \approx \frac{\kappa}{\epsilon^2} \quad \frac{m^2(m^2 - 1)}{m^2 + 1} \tag{39}$$

Upper family: $\lambda \approx \frac{m^2 + 1}{\epsilon^2}$ (40)

These are derived in Appendix B.

Accordingly, the frequencies of the toroidal membrane are divided with a lower family and an upper family of frequencies.

Lower Family

The frequencies and eleastic mode shapes for n = 0, 1, 2, and 3 when $\kappa = 0.002$ are displayed in Figures 4 - 9. The set of three dashed curves on the frequency plots represent "string" frequencies. The mode shapes are shown as distortions of the cross section due to u and w displacement. The v displacement is shown in a separate plot. The complete mode shape is obtained by multiplying the u and w displacements by cos $n\theta$ and the v displacement by sin $n\theta$.

For ϵ small, the lowest mode for each type of vibration, except n = 1, symmetric, is approximated by a ring mode. In the case of the exception, the frequency approaches infinity instead of the "ring" value $\lambda = 2$. The same is true for the second mode of the n = 2 symmetric vibration. Here the frequency would be expected to approach $\lambda = 5$. In both instances the corresponding "ring" modes are of the extensional type. An explanation of these exceptions has not been found.

For ϵ small, frequencies of the higher modes approach the string frequencies.

The most striking feature of the frequency curves is the interaction of the "ring" and "string" modes at approximately the frequencies of the "ring" modes. The result of the interaction is a drastic decrease in frequency of the lowest mode. The decrease in frequency is accompanied by a transition from the overall "ring" to a "string" mode shape associated with deformation of the cross section. The effect of the interaction on the higher modes is to increase the complexity of their mode shapes.

The significant feature of the mode shapes is that they increase in complexity with increasing ϵ: first, through interactions with the "ring" modes and, finally, through local deformations of the cross section. Some interaction areas are exceptions where the mode shapes resemble those of the "ring" modes.

The frequency curves for n = 0, 2 when $\kappa = 0.0001$ are displayed in Figures 20 - 23. These figures show that the interactions between "ring" and "string" modes occur at lower values of ϵ than in the $\kappa = 0.002$ case. The mode shapes for $\kappa = 0.0001$ are similar in nature to those for $\kappa = 0.002$. For this reason they are not displayed.

When the membrane is not prestressed ($\kappa = 0$) it has a continuous frequency spectrum. The range of the spectrum is

$$0 \leq \lambda \leq (1 - \epsilon)^{-2} \quad (41)$$

That is, every frequency in this range is a natural frequency of vibration. The mode shapes are discontinuous. As examples, two mode shapes are shown in Figure 24.

The character of these vibrations is due to the singular nature of the governing differential Equation (23). The frequency range Equation (41) is obtained from the governing Equation (23) by equating to zero that part of the coefficient of u'' which is inside the brackets.

Discontinuous mode shapes are not realistic results. There is evidence that an analysis of the vibrations based upon a nonlinear membrane theory would yield continuous mode shapes. Consider the case $\lambda = 0$. It corresponds to the static deformation of the torus subjected to internal pressure which approaches zero. In this case there are no solutions of the linear membrane equations for which the displacements are continuous (Ref. 5). Studies based upon nonlinear membrane theories (Ref. 4 and 5) show that continuous displacements are possible.

The dependence on prestress ($\kappa = 0$ excluded) of the frequency of the lowest n = 0, symmetric mode is shown in Figure 25. It shows the nonlinear relation between frequency and prestress. The dependence on prestress of all frequencies is such that as the prestress is increased without limit, all frequencies approach infinity.

The modes considered in this section have frequencies of the order of magnitude indicated by Equation (39). Hence, they are considered as constituents of the lower family of frequencies.

Upper Family

The upper family frequencies and mode shapes for $\kappa = 0$ are displayed in Figures 26 - 28. These modes are associated with cross sectional distortions. The frequencies are reasonably well approximated by the string frequencies, except for the second symmetric mode. This frequency curve can be obtained by setting $A_1(\alpha = \pi) = 0$, see Equation (23). Thus, it is a result of the singular nature of Equation (23).

Circumferential Vibrations

The circumferential vibration frequency curves are displayed in Figures 29 and 30, and the mode shapes in Figures 31 and 32. The antisymmetric modes are torsional vibrations about the axis of rotation. The symmetric modes are nontorsional.

For ϵ small, the frequencies of the first symmetric and antisymmetric modes are approximated by

$$2(1 + \nu)\lambda = 1 + O(\kappa)$$

Thus, the circumferential modes are weakly dependent on prestress .

Rigid Body Modes

The rigid body modes ($\lambda = 0$) of the torus are:

1. Displacement parallel to the axis of rotation

$$\bar{u} = \cos \alpha$$

$$\bar{v} = 0$$

$$\bar{w} = \sin \alpha$$

2. Displacement normal to the axis of rotation

$$\bar{u} = \sin \alpha \cos \theta$$

$$\bar{v} = \sin \theta$$

$$w = \cos \alpha \cos \theta$$

3. Rotation about the axis of rotation

$$\bar{u} = \bar{w} = 0$$

$$\bar{v} = r$$

4. Rotation about an axis normal to the axis of rotation

$$\bar{u} = (\epsilon - \cos \alpha) \cos \theta$$

$$\bar{v} = -\epsilon \sin \alpha \sin \theta$$

$$\bar{w} = -\sin \alpha \cos \theta$$

Examples

The ten lowest modes of vibration of two specific structures are computed as examples. Case I is the toroidal membrane idealization of a 150' diameter space station (Ref. 7) ($\epsilon = 1/15$, $\kappa = 0.001875$). Case II is a 24' model torus (Ref. 8) ($\epsilon = 1/3$, $\kappa = 0.00476$). The pertinent parameters of both cases are given in Appendix C.

The frequencies are given in Tables I and II. They are compared with classical ring frequencies (Ref. 6).

The mode shapes of both cases are shown in Figures 33 and 34.

Effect of Centrifugal Forces

Prestress due to centrifugal forces arising from spin about the axis of rotation was considered for Cases I and II. The speed of the spin was such as to cause a 1g acceleration at the outer rim of the torus. Such spinning changes the frequencies of vibration given in Tables I and II by less than one percent.

CONCLUDING REMARKS

The results of the numerical analysis show that there are three groups of modes of vibration:

1. Lower family, for which the modes of classical ring theory, and those of the prestressed circular string are limiting cases;

2. Upperfamily, whose frequencies are reasonably well approximated by the upper family of frequencies of the prestressed circular string;

3. Circumferential modes.

The frequencies of the lower family modes depend strongly on the intensity of prestress. The circumferential modes are practically independent of prestress.

The "ring" and "string" modes interact causing a decrease in frequency that is associated with cross sectional distortion.

The study of the upper family modes should be extended to include non-axisymmetrical modes of vibration and the effect of prestress.

ACKNOWLEDGMENT

The author acknowledges the work of Professor B. Budiansky, whose contributions in this investigation were notable.

Appendix A

COEFFICIENTS OF DIFFERENTIAL EQUATIONS

Define the following quantities:

$$k = (1-\nu^2)\kappa$$

$$S = \frac{\epsilon \sin\alpha}{1-\epsilon\cos\alpha}$$

$$C = \frac{\epsilon\cos\alpha}{1-\epsilon\cos\alpha}$$

$$N = \frac{\epsilon n}{1-\epsilon\cos\alpha}$$

$$M = 1 + 2\Gamma\,(1-\epsilon\cos\alpha)^2$$

$$Q = \epsilon^2(1-\nu^2)\lambda - 1 + \left(2\nu - \frac{3k}{2}\right)C - \left(1+\frac{k}{2}M\right)C^2 - \frac{k}{2}MN^2$$

$$T_1 = 1 - \left(\nu - \frac{k}{2}\right)C$$

$$T_2 = S\left[\nu - k - \left(1+\frac{k}{2}M\right)C\right]$$

$$T_3 = N\left[\nu - k - (1+kM)C\right]$$

$$T_4 = 1 + k - \left(\nu - \frac{k}{2}\right)C$$

$$T_5 = N\left[k - \nu + (1+k)C\right]$$

$$T_6 = QS\left(1+\frac{k}{2}M\right)(1+C) - T_4 Q'$$

The derivatives of M, Q, T_1, T_2 and T_3 are:

$$M' = 4\epsilon\Gamma\,(1-\epsilon\cos\alpha)\sin\alpha$$

$$Q' = \left[2\left(1+\frac{k}{2}M\right)C - \left(2\nu - \frac{3k}{2}\right)\right]S(1+C) + kMN^2S - \frac{k}{2}M'(N^2+C^2)$$

$$T_1' = S\left(\nu - \frac{k}{2}\right)(1+C)$$

$$T_2' = \left[\nu - k - \left(1+\frac{k}{2}M\right)C\right](C-S^2) + S\left[S\left(1+\frac{k}{2}M\right)(1+C) - \frac{k}{2}M'C\right]$$

$$T_3' = NS\left[(1-\nu) + k(1+M) + 2(1+kM)C\right] - kM'NC$$

The elements of the A, B and C matrices are:

$$A_{11} = Q\left\{(1-\nu^2)\ (\epsilon^2\lambda - C^2) - k\left[(1-\nu)\,C - \left(1+\frac{1}{2}\,C\right)\epsilon^2(1-\nu^2)\lambda + \right.\right.$$
$$\left.\left. + \frac{1}{2}\,M\,(N^2+C^2)\left(1+k+\frac{k}{2}\,C\right) + C\left(1+\frac{1}{2}\,C\right)\left(k+C\right)\right]\right\}$$

$$A_{13} = kQ\,T_4\left(1+\frac{1}{2}\,C\right)$$

$$A_{22} = Q\left[\frac{1}{2}\,(1-\nu) + k\left(1+\frac{1}{2}\,C\right)\right]$$

$$A_{31} = QT_1$$

$$A_{33} = kQ\left(1+\frac{1}{2}\,C\right)$$

$$A_{12} = A_{21} = A_{23} = A_{32} = 0$$

$$B_{11} = Q\left[QS\left(1+\frac{k}{2}\,M\right) + T_4\ (T_1' + T_2)\right] + T_1\,T_6$$

$$B_{12} = Q\left[\frac{1}{2}(1+\nu)\,NQ + T_3\,T_4\right]$$

$$B_{13} = k\left[T_6\left(1+\frac{1}{2}\,C\right) - \frac{1}{2}\,Q\,T_4 S\,(1-M+C)\right]$$

$$B_{21} = T_1\,T_5 - \frac{1}{2}\,(1+\nu)\,QN$$

$$B_{22} = \frac{1}{2}\,QS\,(1-\nu+k\,M)$$

$$B_{23} = k\,T_5\left(1+\frac{1}{2}\,C\right)$$

$$B_{31} = Q(T_1' + T_2) - Q'\,T_1$$

$$B_{32} = QT_3$$

$$B_{33} = -k\left[Q'\left(1+\frac{1}{2}\,C\right) + \frac{1}{2}\,QS\,(1-M+C)\right]$$

$$C_{11} = Q^2\left[\nu\,C - S^2 - \frac{1}{2}\,(1-\nu)\,N^2 - \frac{k}{2}\,M\,(N^2+S^2) + \epsilon^2(1-\nu^2)\lambda\right] + QT_4\,T_2' + T_2\,T_6$$

$$C_{12} = -QNS\left[\frac{1}{2}\ (3-\nu) + kM\right] + QT_4\,T_3' + T_3\,T_6$$

$$C_{13} = \frac{k}{2}\left\{ Q\,T_4\left[M\,(C - S^2) + M'S \right] - Q^2 C + T_6\,MS \right\}$$

$$C_{21} = T_2\,T_5 - \left[\frac{1}{2}\,(3-\nu) + kM \right] QNS$$

$$C_{22} = Q\left[\epsilon^2\,(1-\nu^2)\,\lambda - N^2 - \frac{1}{2}\,(1-\nu)\,(C+S^2) - \frac{k}{2}\,M\,(N^2+S^2+C^2) - kC \right] + T_3 T_5$$

$$C_{23} = \frac{k}{2}\,T_5\,MS$$

$$C_{33} = \frac{k}{2}\,Q\left[M(C-S^2) + M'S \right] - \frac{k}{2}\,Q'\,MS + Q^2$$

The coefficients of the differential Equation (23) are:

$$A_1 = \epsilon^2\,(1-\nu^2)\,\bar{Q}$$

$$A_2 = \bar{Q}^2 S + \bar{Q}\,S\,(1-\nu C)\left[(\nu - C) + \nu\,(1+C) \right] + S(1-\nu C)\,(1+C)\left[\bar{Q} + 2(1-\nu C)\,(\nu - C) \right]$$

$$A_3 = \bar{Q}^2\left[\nu C - S^2 + \epsilon^2(1-\nu^2)\,\lambda \right] + \bar{Q}(1-\nu C)\left[(\nu - C)\,(C - S^2) + S^2\,(1+C) \right] \pm S^2(\nu - C)\,(1 \pm C)\left[\bar{Q} + 2\,(1-\nu C)\,(\nu - C) \right]$$

where $\bar{Q} = \epsilon^2(1-\nu^2)\,\lambda - 1 + 2\,\nu\,C - C^2$

The coefficients of the differential Equation (24) are:

$$B_1 = 1 + k^*\,(2 + C)$$

$$B_2 = S(1 + k^*\,M)$$

$$B_3 = 2(1+\nu)\,\epsilon^2\lambda - (C + S^2) - k^*\,(MS^2 + MC^2 + 2C)$$

where $k^* = (1+\nu)\,\kappa$

Appendix B

VIBRATION OF THE PRESTRESSED CIRCULAR STRING

The analysis is based upon the membrane equations of Ref. (2). For the prestressed circular string they are:

Equilibrium

$$\begin{aligned} N_s' + S_s (E_s' - \phi_s) + pR\phi_s + \rho hR\omega^2 U = 0 \\ N_s + S_s (E_s + \phi_s') - pRE_s - \rho hR\omega^2 W = 0 \end{aligned} \tag{B1}$$

Strain - Displacement

$$\begin{aligned} E_s &= \frac{1}{R} (U' + W) \\ \phi_s &= \frac{1}{R} (-W' + U) \end{aligned} \tag{B2}$$

Constitutive Relation

$$N_s = EhE_s \tag{B3}$$

The prestress is

$$S_s = pR \tag{B4}$$

Substitution of Equations (B2-B4) into (B1) yields

$$\begin{aligned} (1+\kappa) U'' + \epsilon^2 \lambda u + (1+\kappa) W' = 0 \\ (1+\kappa) U' - \kappa W'' + (1-\epsilon^2 \lambda) W = 0 \end{aligned} \tag{B5}$$

The solutions of Equations (B5) are:

$$U = \sum_{n=0}^{\infty} a_n \sin m\alpha$$
$$W = \sum_{n=0}^{\infty} b_n \cos m\alpha \qquad \text{(B6)}$$

With this solution, the frequency equation can be obtained from Equations (B5) in the usual manner

$$(E^2\lambda)^2 - (1 + m^2 + 2\kappa m^2)\ (\epsilon\lambda) + \kappa(1+\kappa)\, m^2 (m^2 - 1) = 0 \qquad \text{(B7)}$$

The roots of the frequency equation are approximately

$$\lambda \approx \frac{\kappa}{\epsilon^2} \quad \frac{m^2 (m^2 - 1)}{m^2 + 1} \qquad \text{(B8)}$$

$$\lambda \approx \frac{m^2 + 1}{\epsilon^2} \qquad \text{(B9)}$$

where κ has been neglected in presence of unity.

Appendix C

STRUCTURAL PARAMETERS

The structural parameters of Case I (Ref. 7) and Case II (Ref. 8, 9) are given below:

		Case I	Case II
R	=	5'	8'
$\frac{R}{\epsilon}$	=	75'	24'
h	=	0.032"	0.080"
p	=	10 psi	7 psi
E	=	10^7 psi	1.763×10^6 psi
ν	=	0.3	0
ρg	=	0.1 #/in^3	0.0217 #/in^3
κ	= $\frac{pR}{Eh}$ =	0.001875	0.00476
ϵ	=	1/15	1/3
Γ	= $\frac{\rho h R^2 \Omega^2}{pR\epsilon^2}$ =	0.00450	0.000558

Wall thickness of Case I is based on a yield stress of 65,000 psi and a design pressure of 30 psi. Young's Modulus of Case II is for individual chords of the filament cage. Ω produces a 1g acceleration at the outer rim.

REFERENCES

1. A general theory of vibrations of shells to be published by Bernard Budiansky.

2. Timoshenko, S., Theory of Plates and Shells, McGraw-Hill Book Co., Inc., New York, 1940.

3. Jordan, P. F., "Stresses and Deformations of the Thin-Walled Pressurized Torus," J. Aerospace Sci. 29, 213-225, (Feb. 1962).

4. Sanders, J. L., Jr., and A. A. Liepins, "Toroidal Membrane Under Internal Pressure," AIAA Journal, 1(9), 2105-2110, (Sept. 1963).

5. Budiansky, B. and P. P. Radkowski, "Numerical Analysis of Unsymmetrical Bending of Shells of Revolution," AIAA Journal, 1(8), 1833-1842, (Aug. 1963).

6. Love, A. E. H., The Mathematical Theory of Elasticity, Dover Publications, New York, 1927.

7. Zender, G. W. and T. R. Davidson, "Structural Requirements of Large Manned Space Stations, in Report on the Research and Technological Problems of Manned Rotating Spacecraft," NASA TN D-1504, (Aug. 1962).

8. Osborne, R. S. and G. P. Goodman, "Materials and Fabrication Techniques for Manned Space Stations, in Report on the Research and Technological Problems of Manned Rotating Spacecraft," NASA TN D-1504, (Aug. 1962).

9. Geometry and Structural Analysis of the 24-foot C-Annulus Space Station, Goodyear Aircraft Corporation, Engineering Memorandum Report, August 3, 1961.

Table I Frequencies of Case I

Mode Number	Fourier Index	Type	Frequency Cps	Ring Frequency Cps
1	2	Antisymmetric	3.67	4.27
2	2	Symmetric	3.77	4.39
3	3	Antisymmetric	10.07	12.2
4	3	Symmetric	10.13	12.4
5	4	Antisymmetric	18.4	23.6
6	4	Symmetric	18.5	23.8
7	0	Antisymmetric	19.5	24.6
8	5	Antisymmetric	27.5	38.3
9	5	Symmetric	27.6	38.5
10	1	Antisymmetric	27.7	32.7

Table II Frequencies of Case II

Mode Number	Fourier Index	Type	Frequency Cps	Ring Frequency Cps
1	0	Antisymmetric	2.63	6.92
2	2	Antisymmetric	2.70	6.01
3	2	Symmetric	2.97	6.19
4	3	Antisymmetric	5.03	17.2
5	3	Symmetric	5.11	17.5
6	4	Symmetric	6.720	33.3
7	4	Antisymmetric	6.722	33.6
8	3	Antisymmetric	7.85	—
9	2	Antisymmetric	7.86	—
10	2	Symmetric	7.87	—

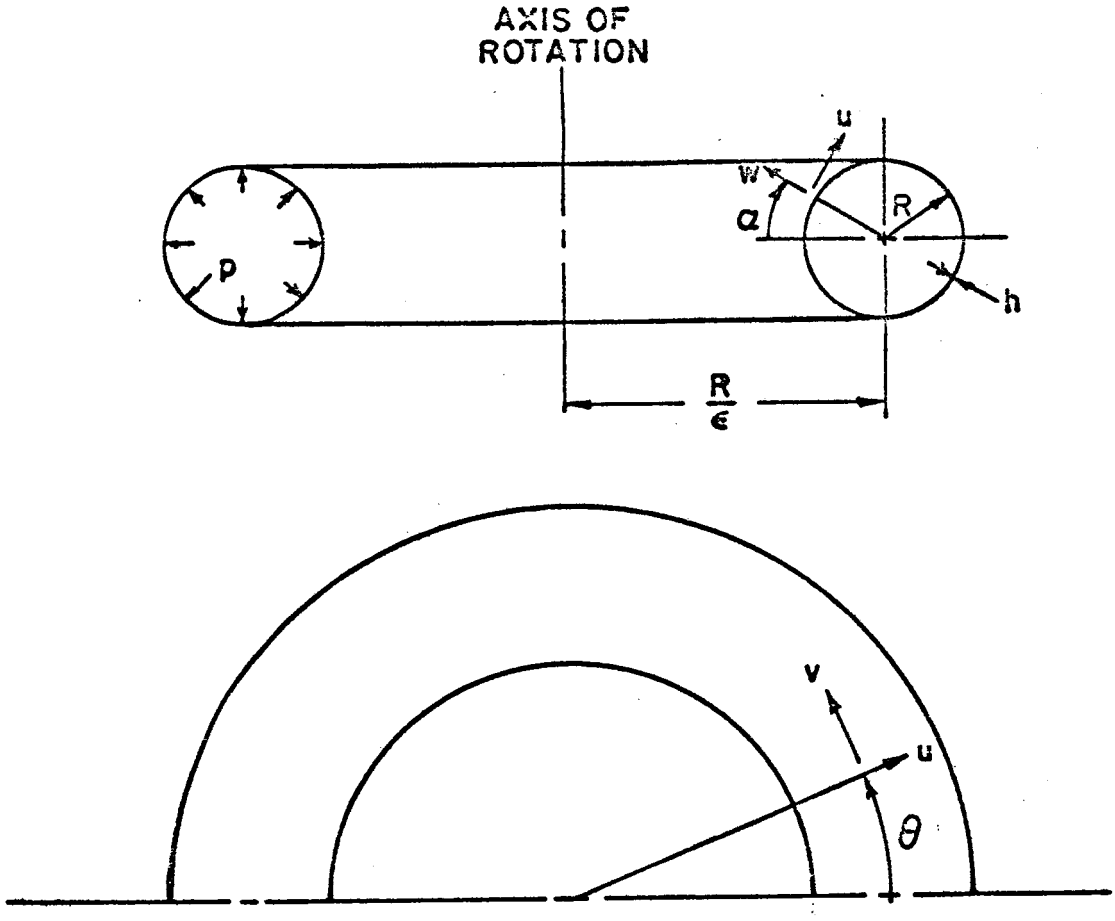

FIGURE 1: GEOMETRY AND NOTATION

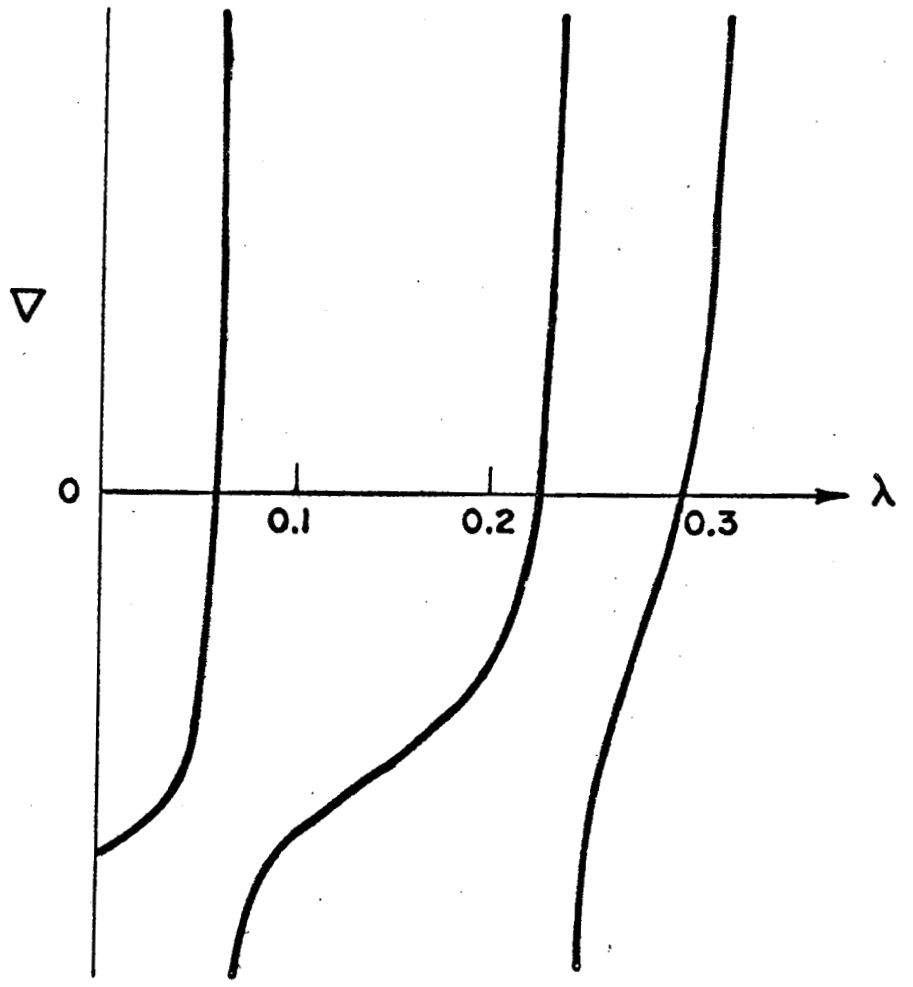

FIGURE 2: TYPICAL PLOT OF THE FREQUENCY EQUATION

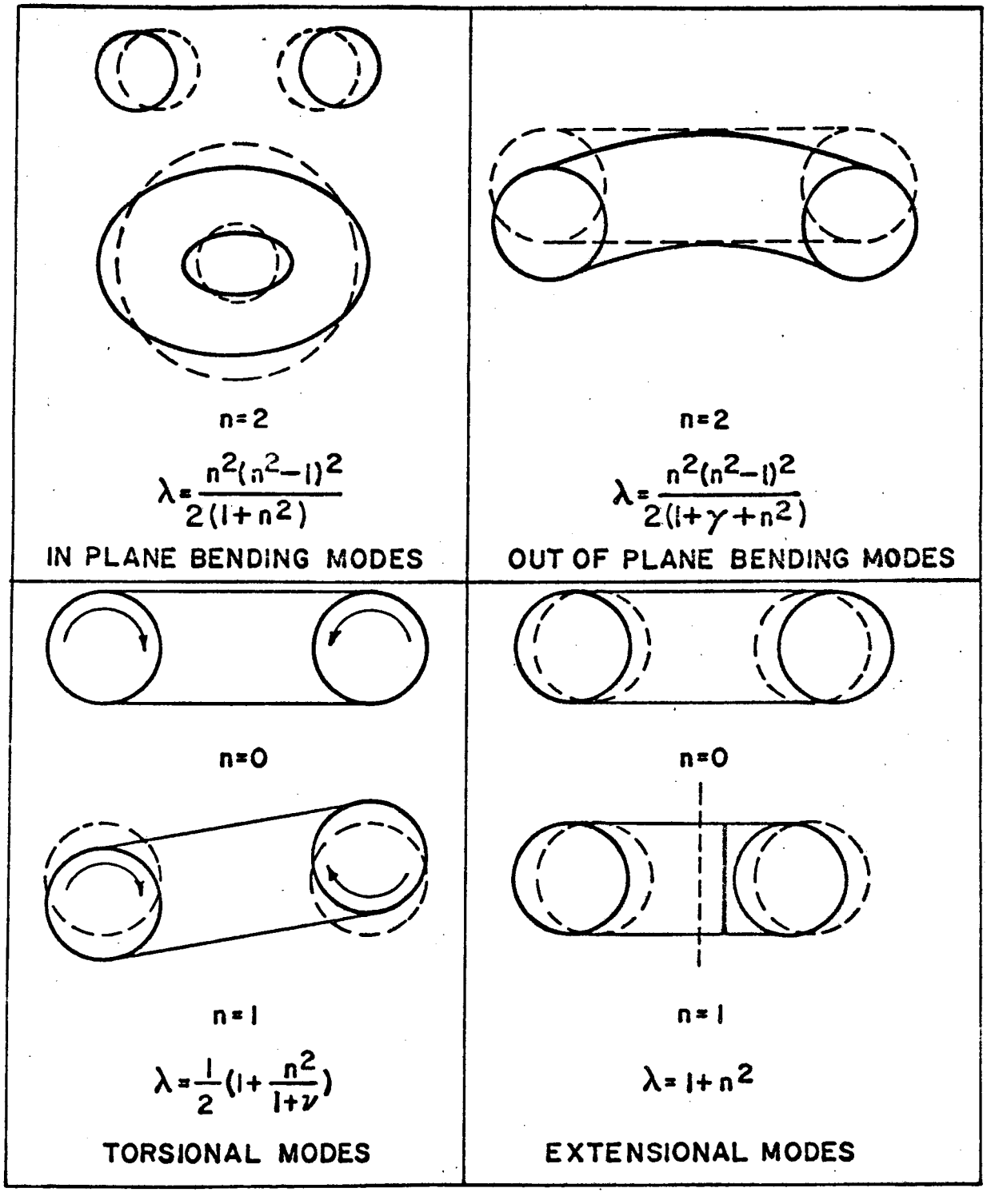

FIGURE 3: RING FREQUENCIES AND MODE SHAPES

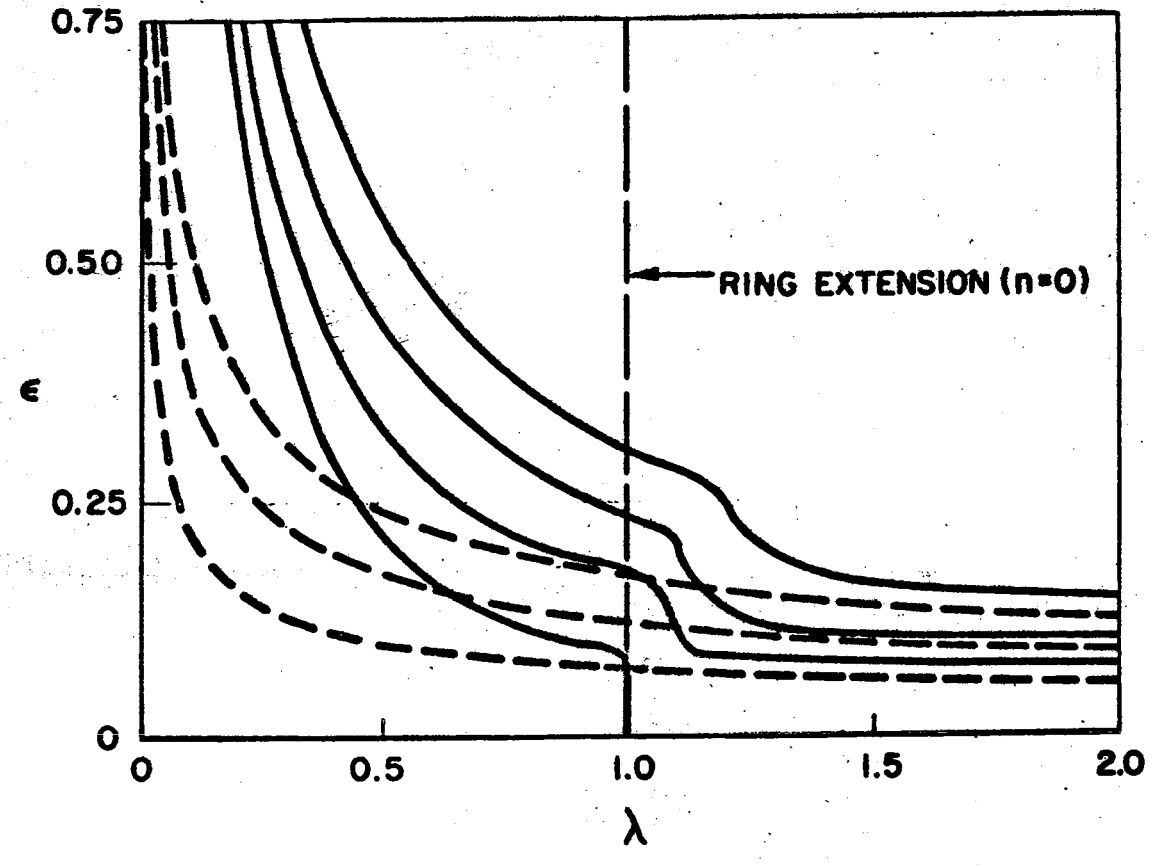

FIG.4: AXISYMMETRIC MODES, SYMMETRIC, $K = 0.002$

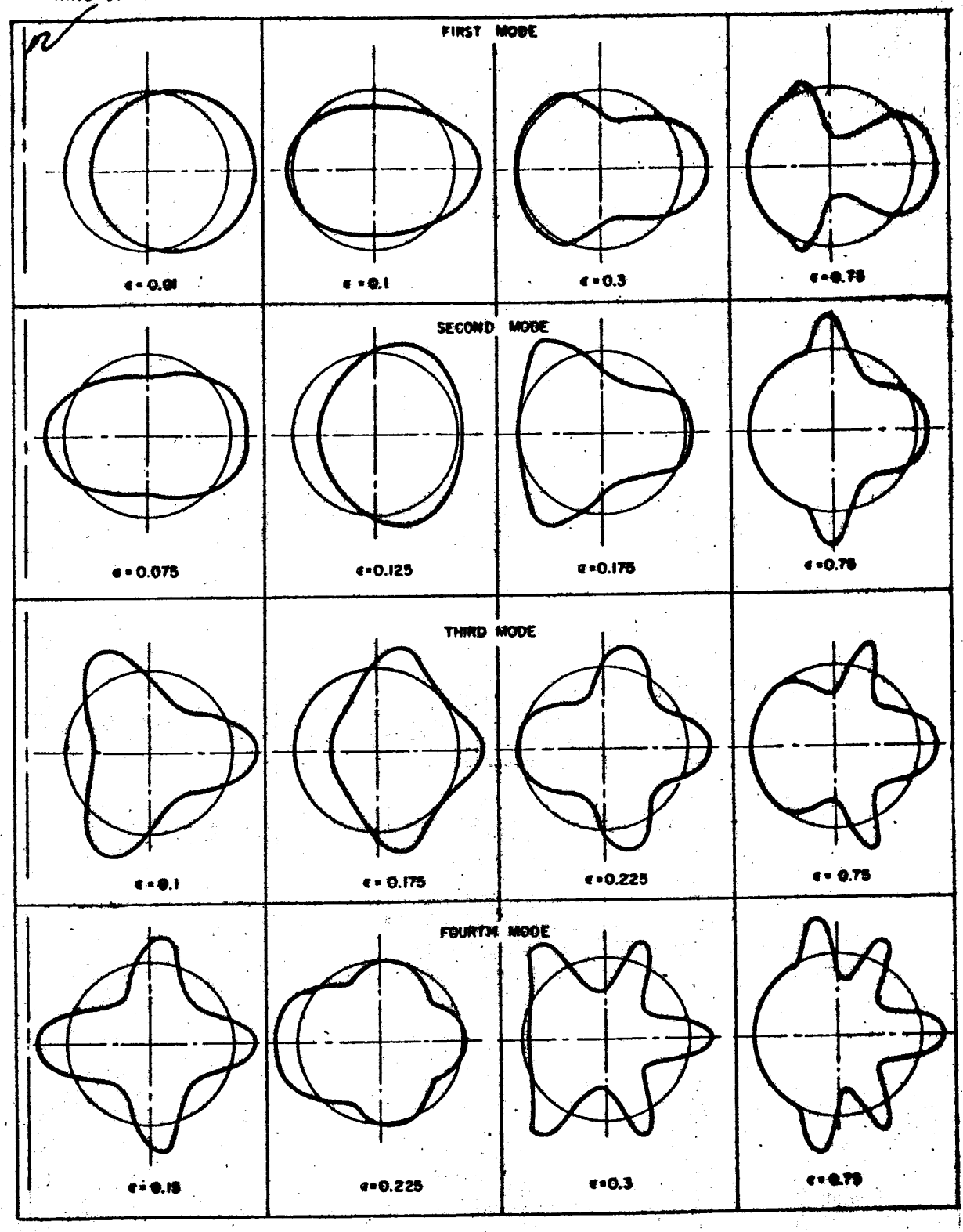

FIGURE 5 : AXISYMMETRIC MODE SHAPES, SYMMETRIC, $R = 0.002$

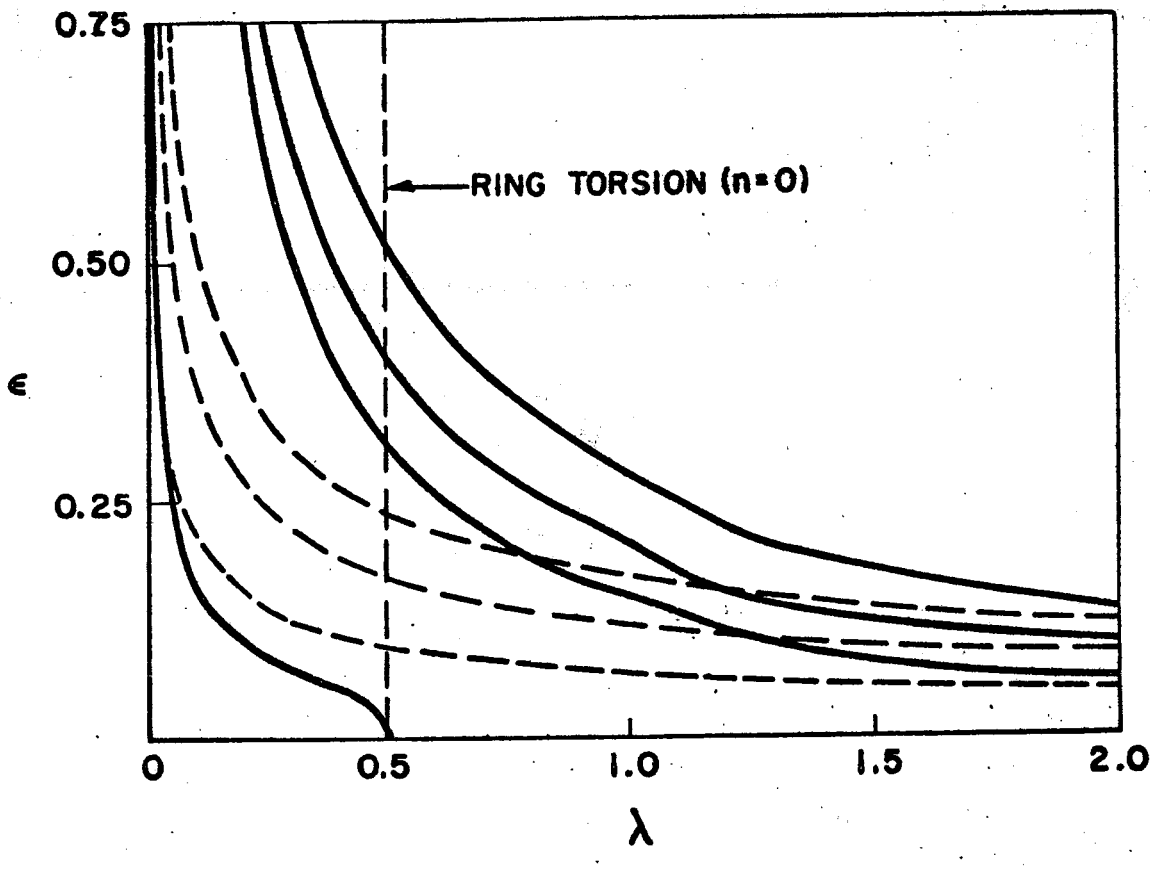

FIG. 6: AXISYMMETRIC MODES, ANTISYMMETRIC, $\kappa = 0.002$

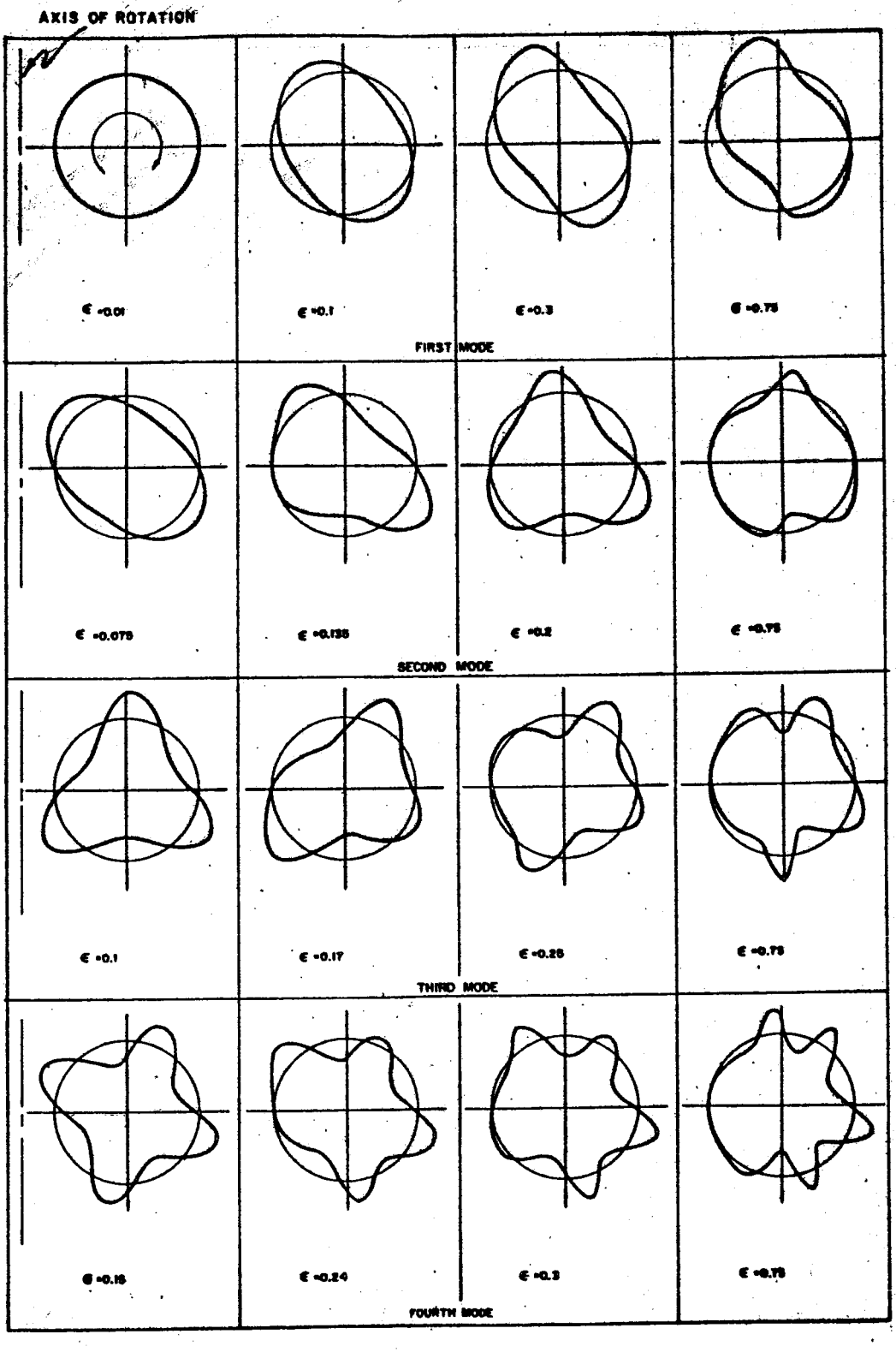

FIGURE 7; AXISYMMETRIC MODE SHAPES, ANTISYMMETRIC, $\alpha' = 0.002$

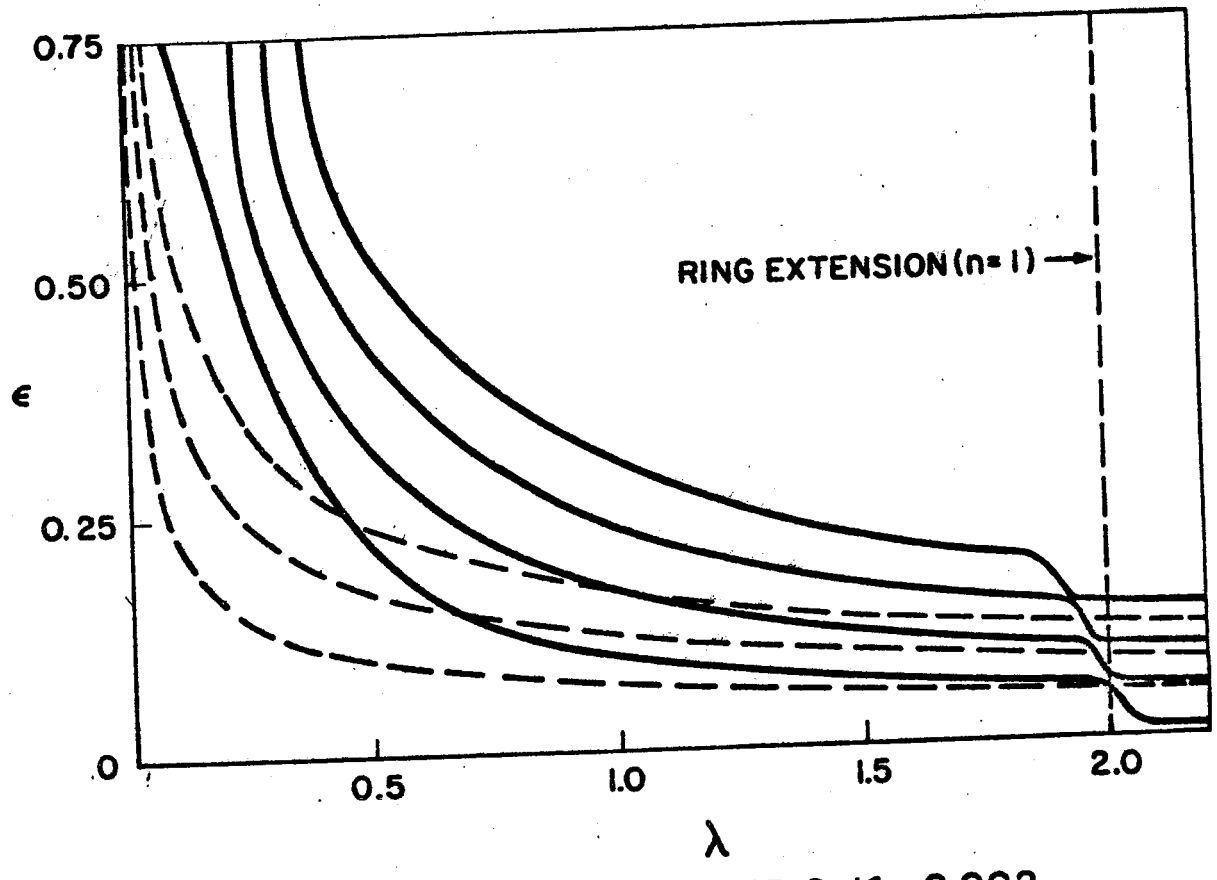

FIG. 8: n = 1 MODES, SYMMETRIC, $\kappa = 0.002$

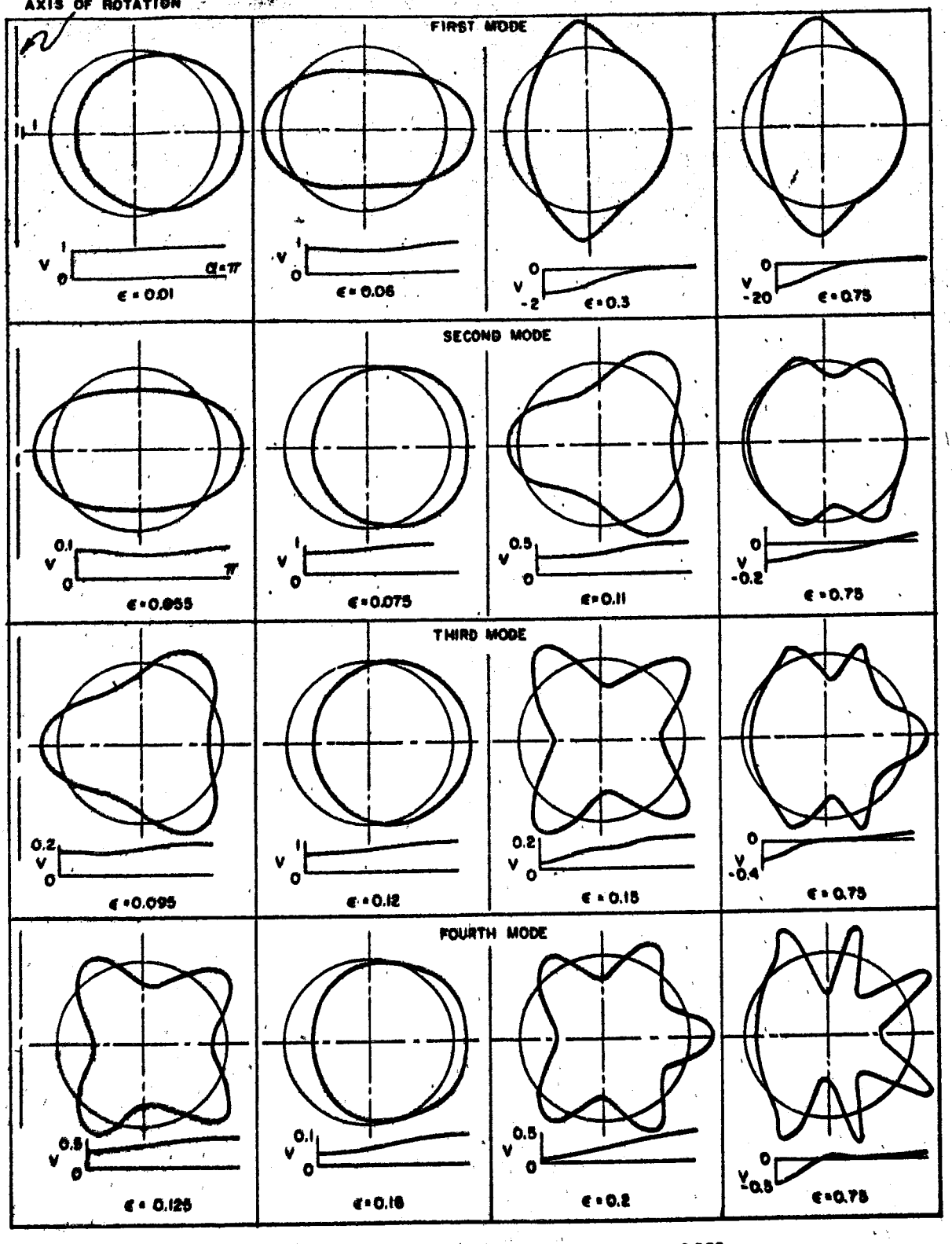

FIGURE 9 n=1 MODE SHAPES, SYMMETRIC, $\kappa = 0.002$

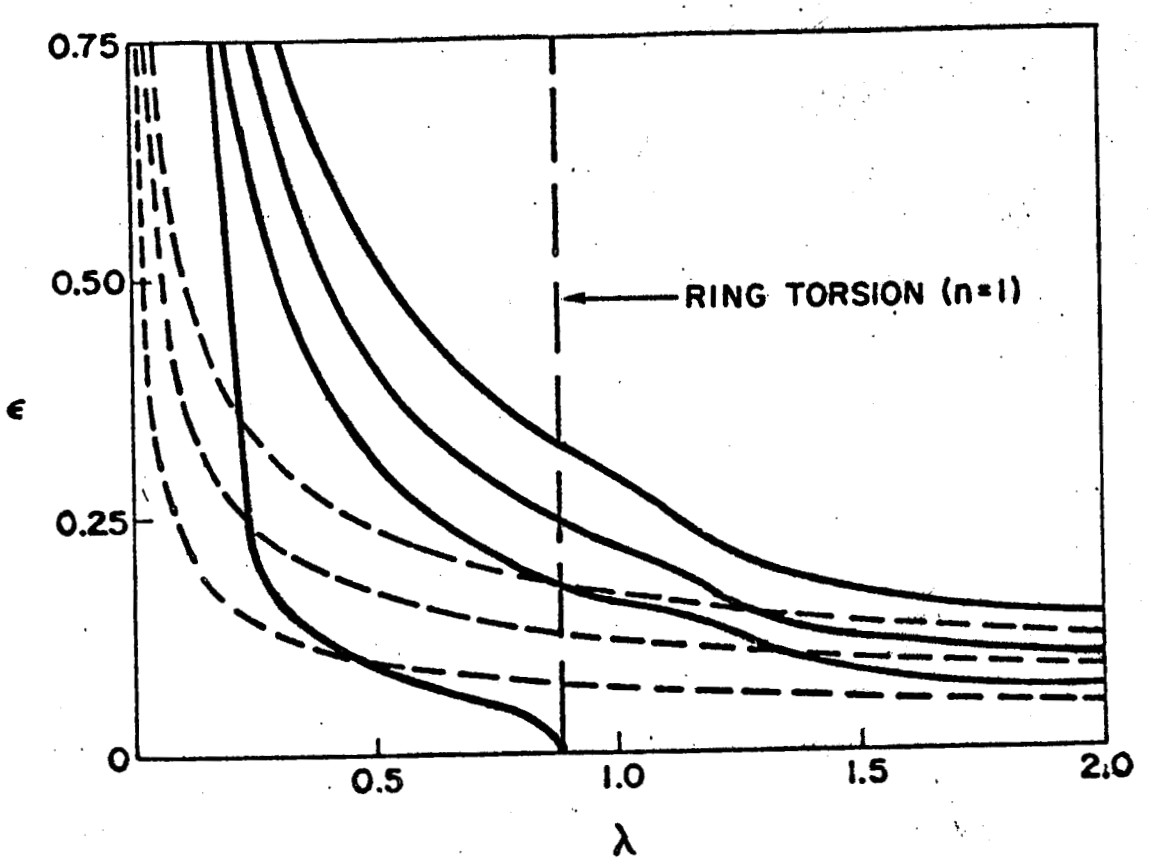

FIGURE 10: n = 1 MODES, ANTISYMMETRIC, $K = 0.002$

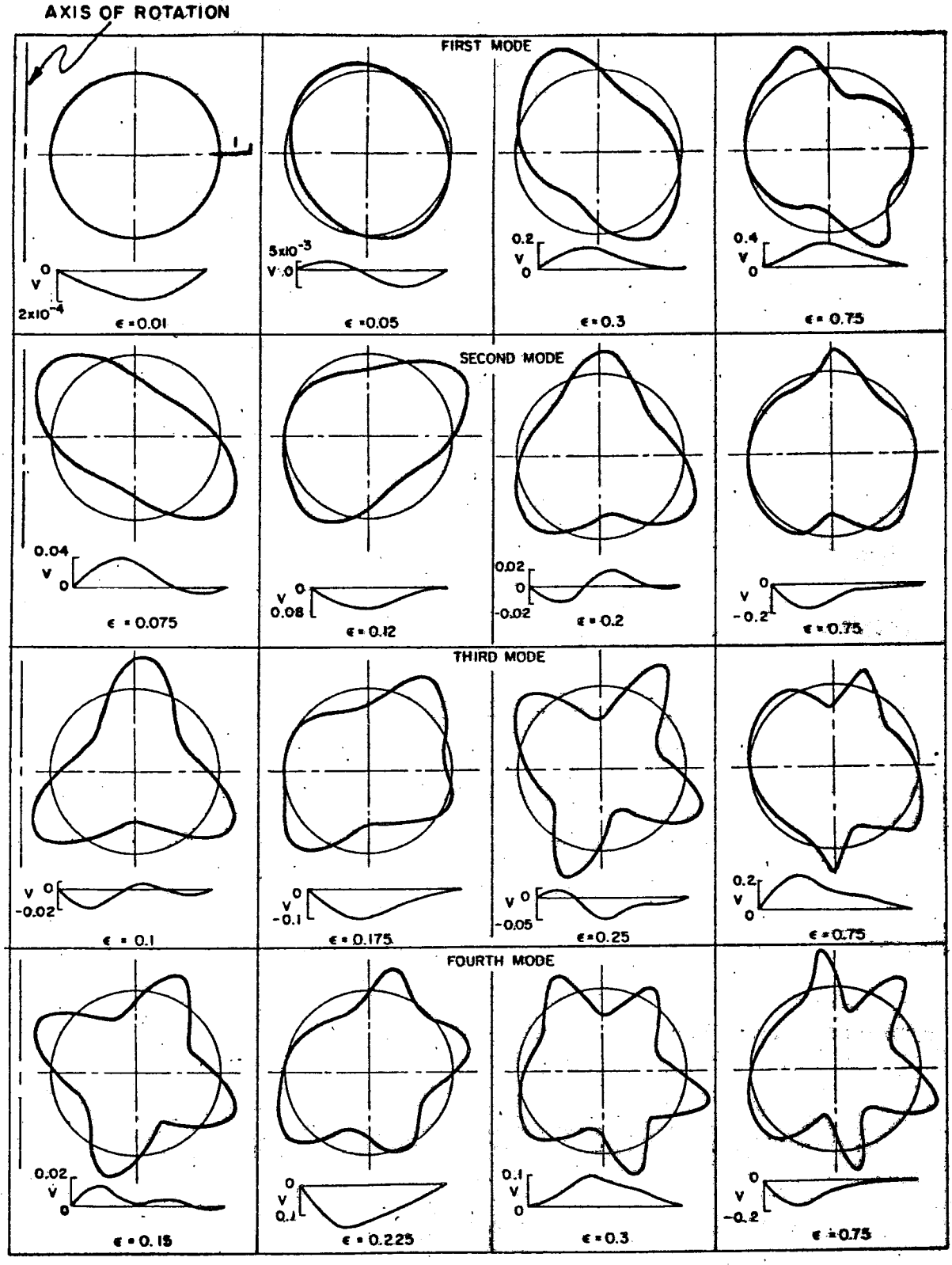

FIGURE 11 : n = 1 MODE SHAPES, ANTISYMMETRIC, κ = 0.002

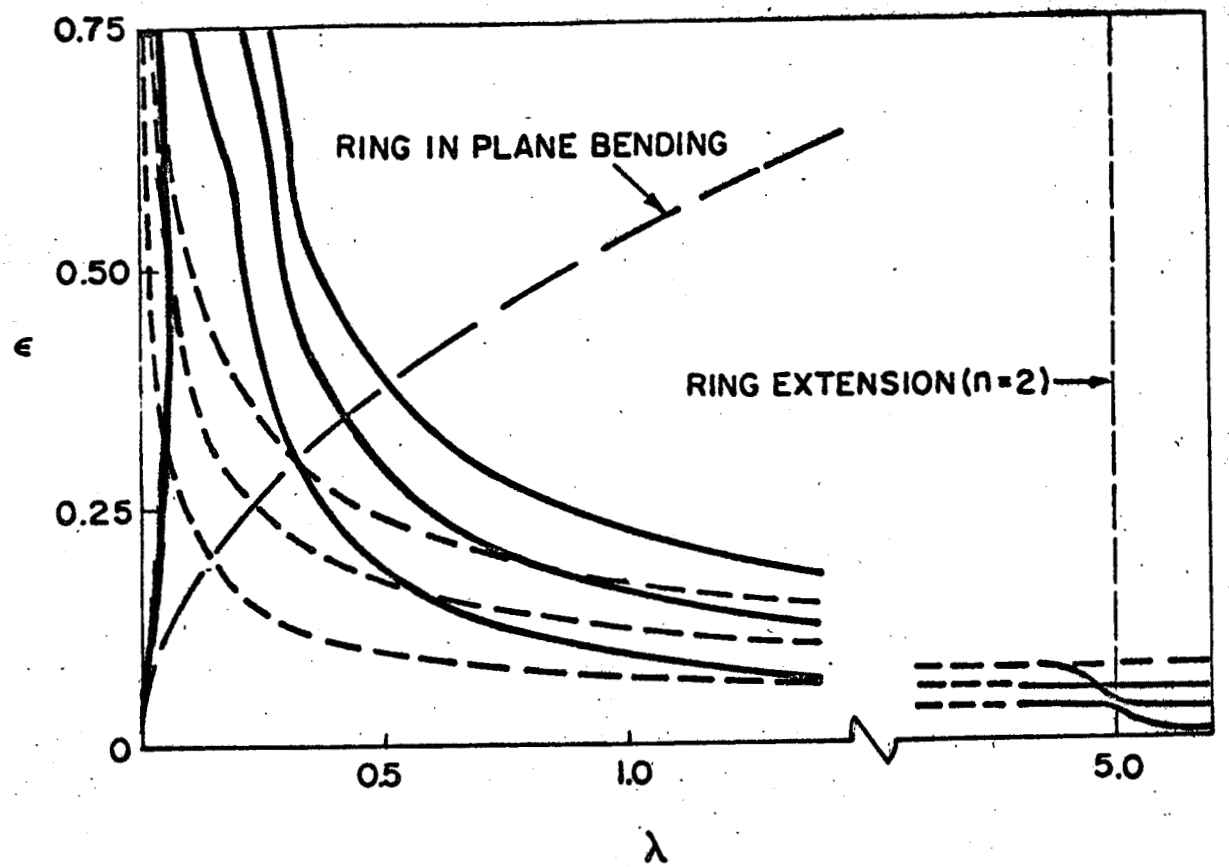

FIGURE 12: n = 2 MODES, SYMMETRIC, $\kappa = 0.002$

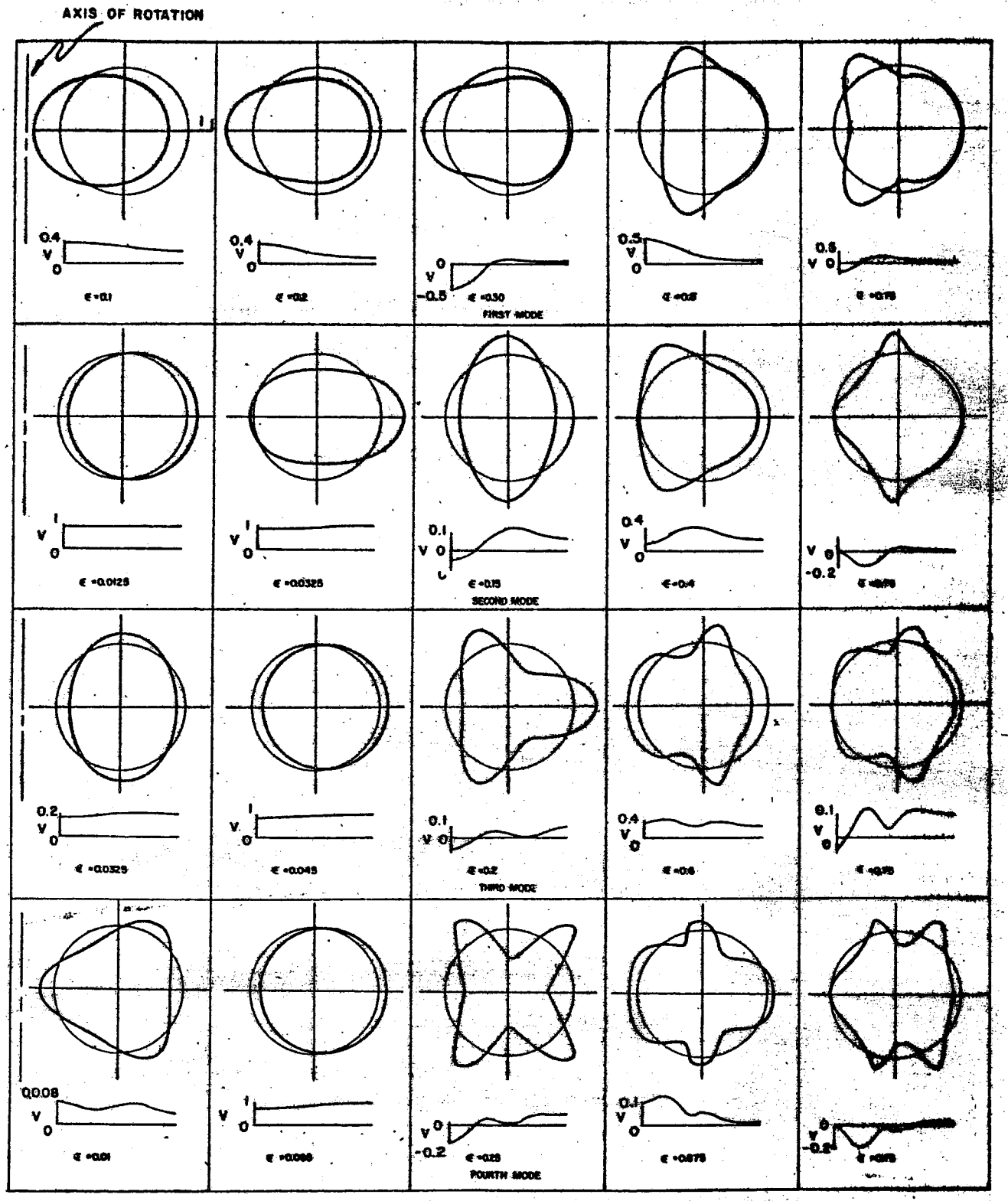

FIGURE 13 n=2 MODE SHAPES SYMMETRIC, κ =0.002

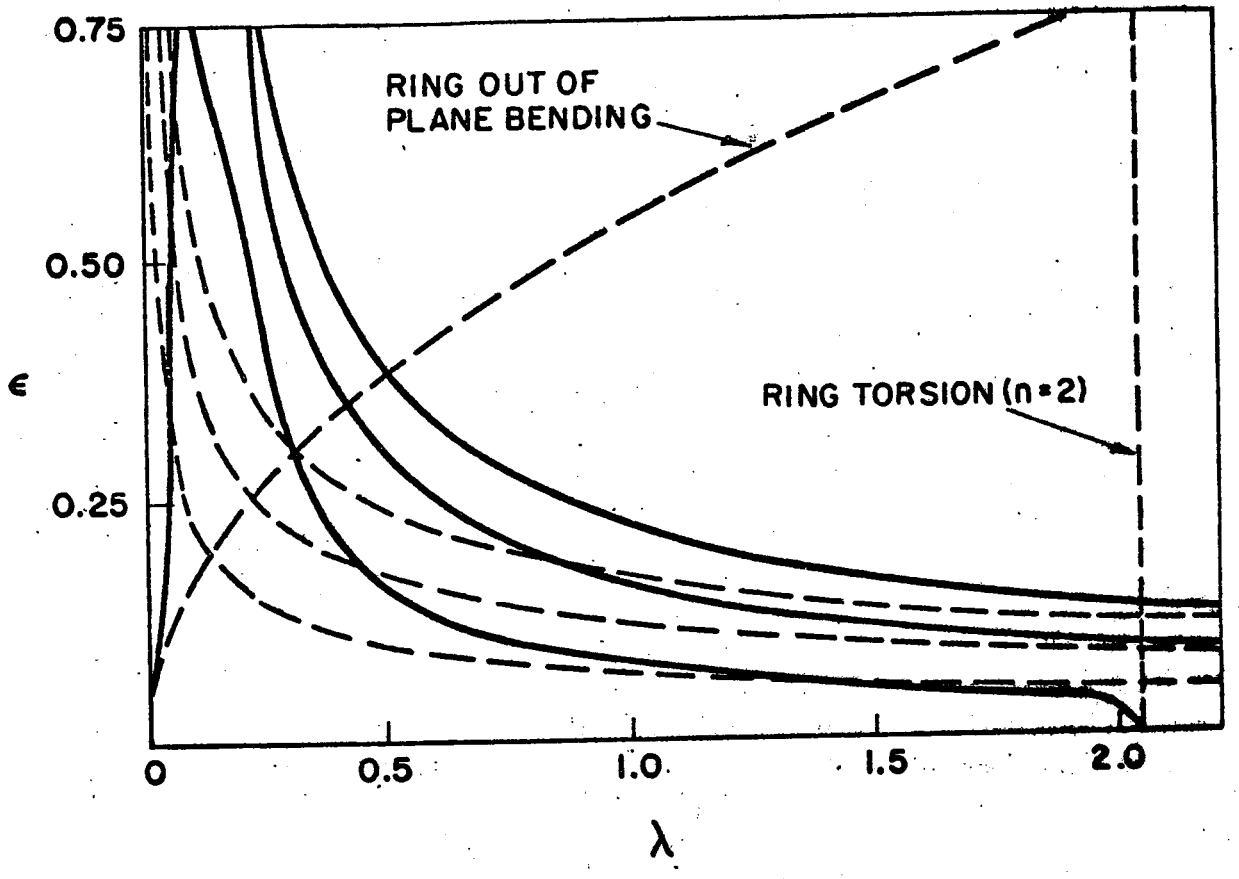

FIG. 14: n=2 MODES, ANTISYMMETRIC, $K = 0.002$

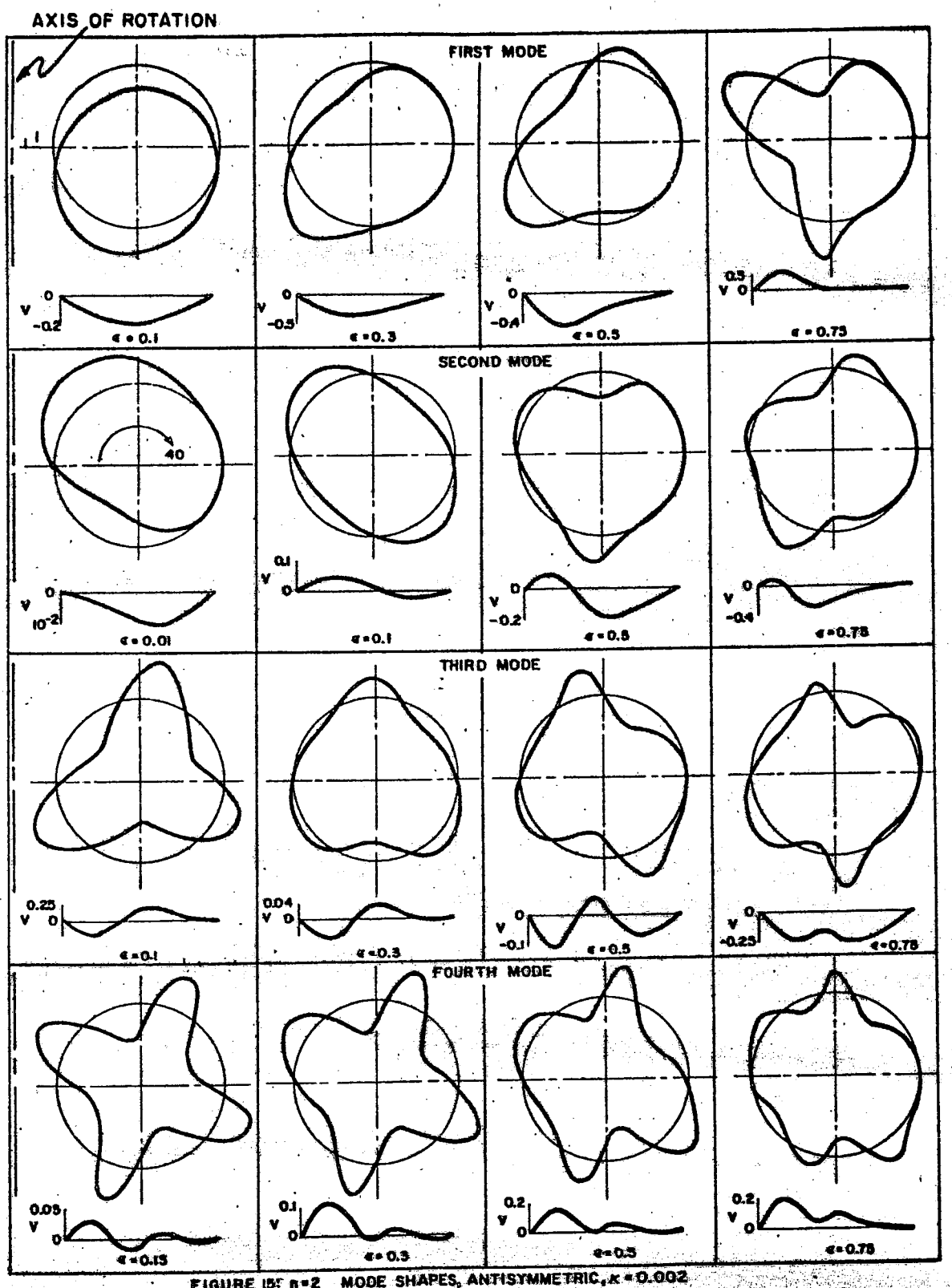

FIGURE 15: n=2 MODE SHAPES, ANTISYMMETRIC, $\kappa = 0.002$

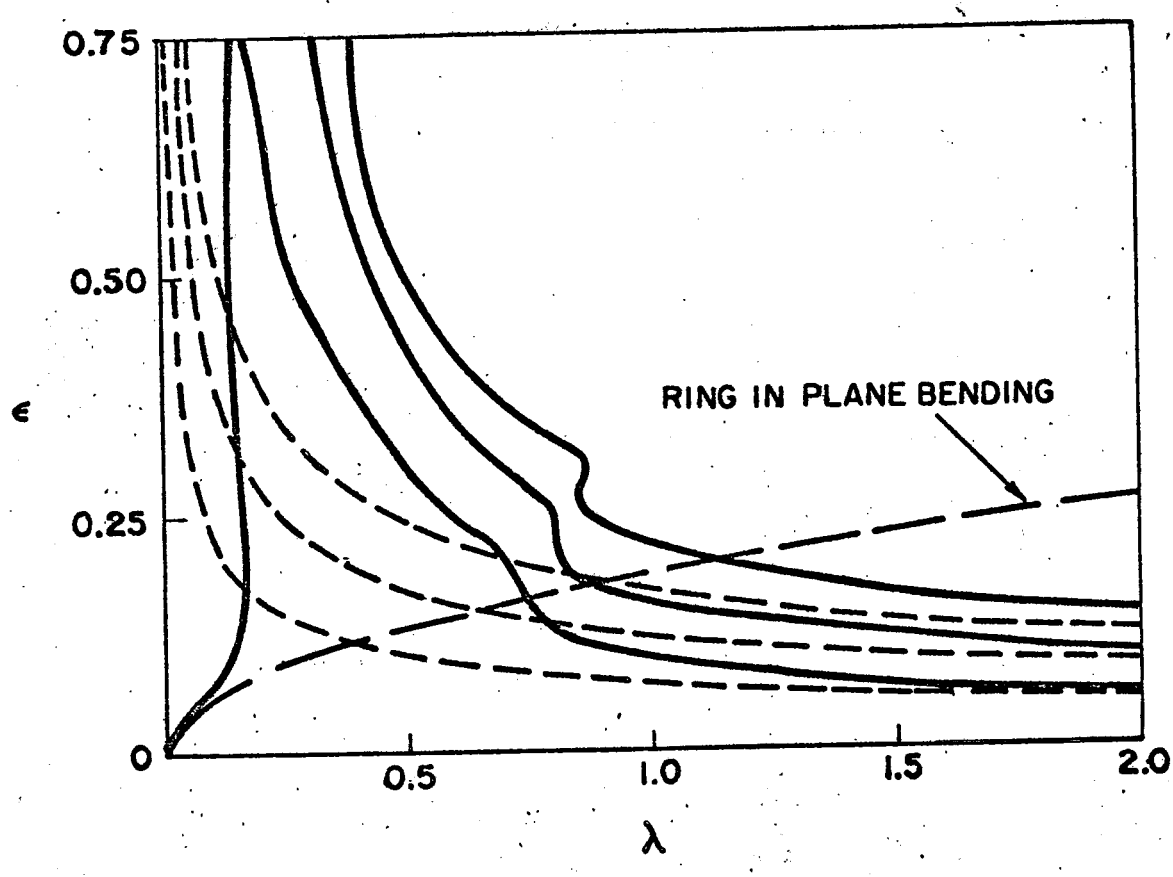

FIGURE 16: n=3 MODES, SYMMETRIC, $K = 0.002$

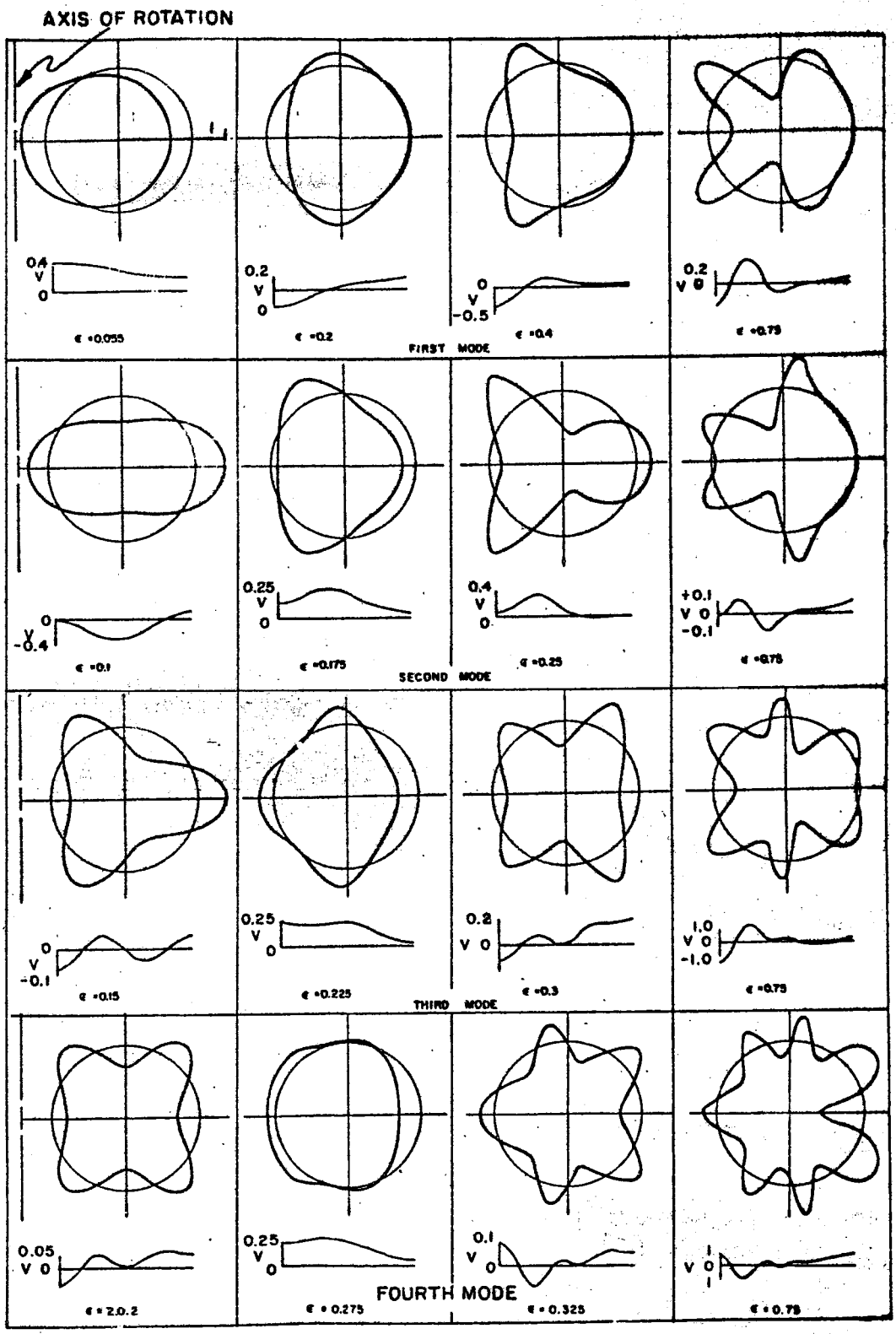

FIGURE 17: n = 3 MODE SHAPES, SYMMETRIC, $K = 0.002$

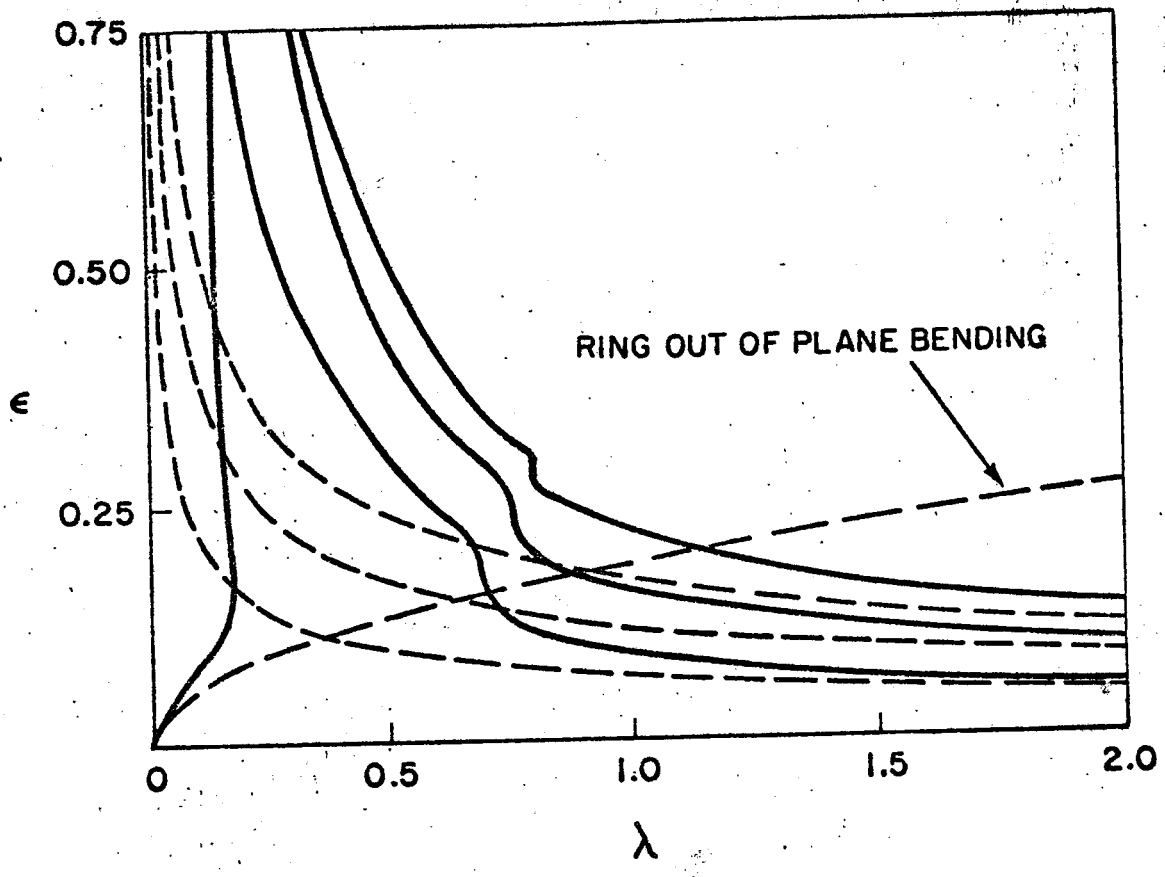

FIG. 18: n = 3 MODES, ANTISYMMETRIC, $K = 0.002$

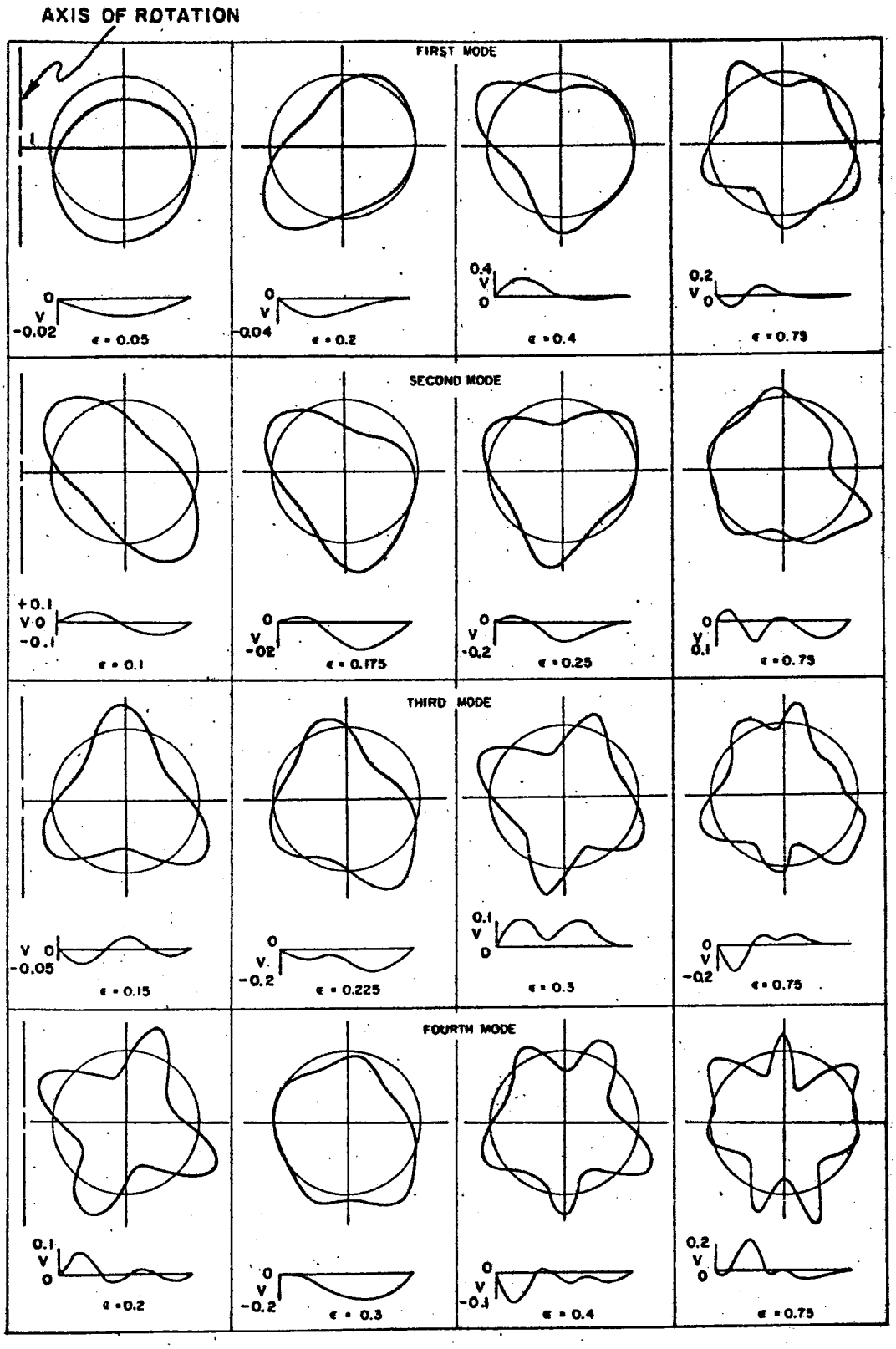

FIGURE 19: n = 3 MODE SHAPES, ANTISYMMETRIC, $K = 0.002$

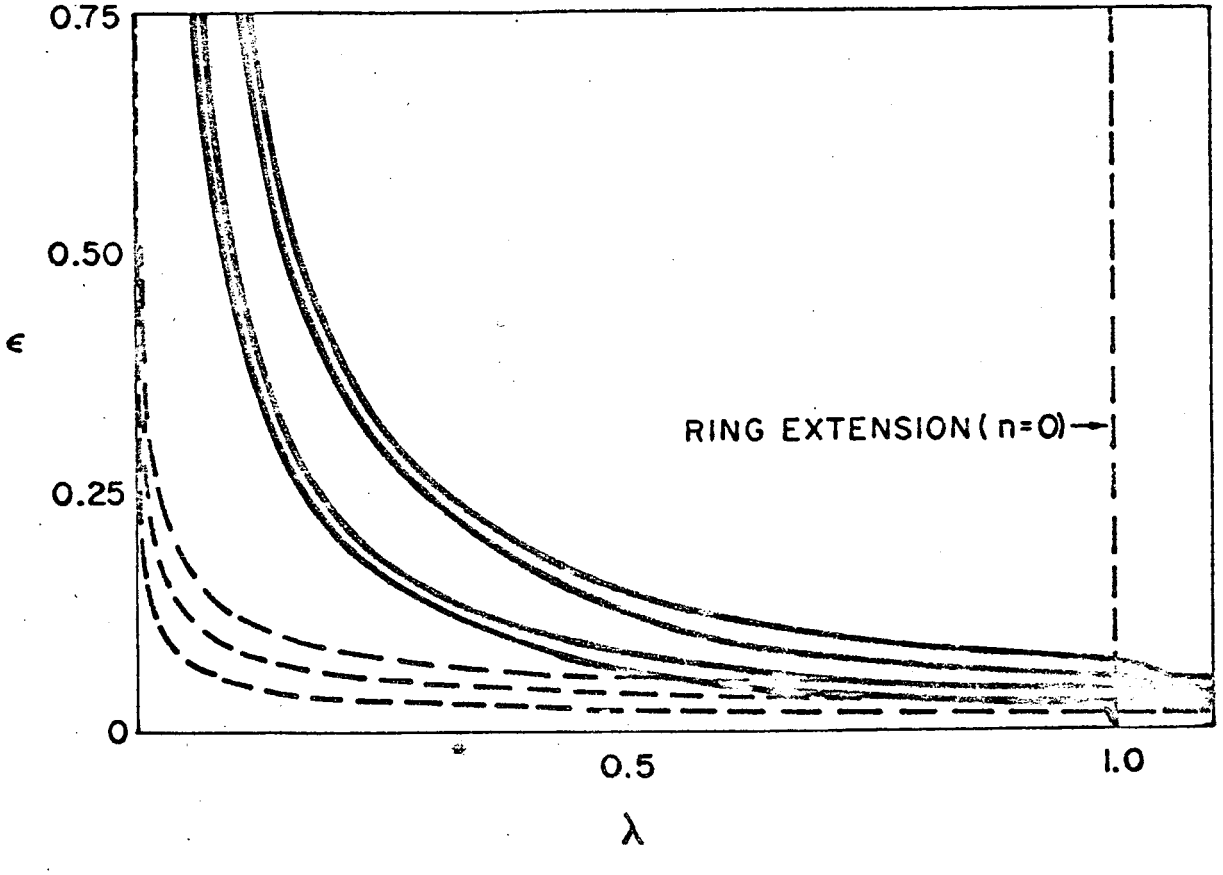

FIGURE 20: AXISYMMETRIC MODES, SYMMETRIC, $K = 0.0001$

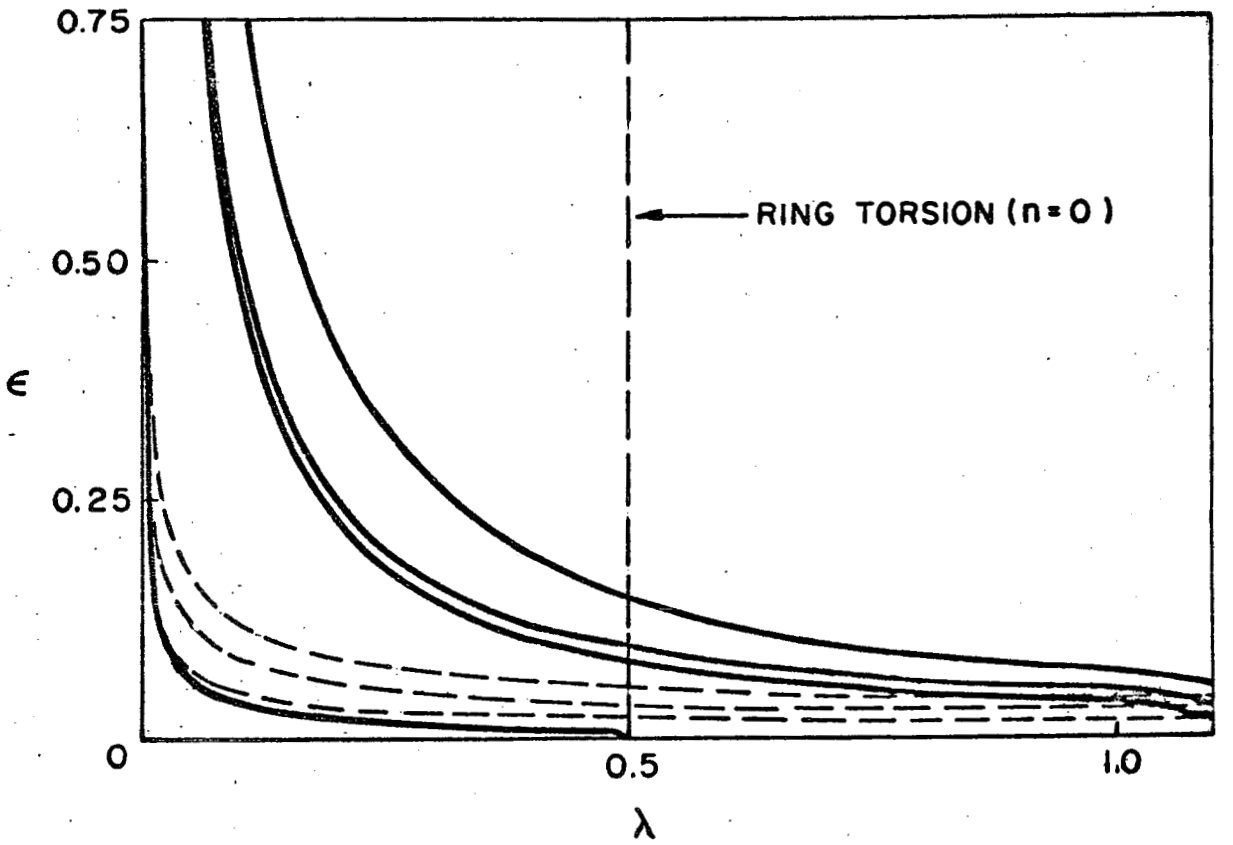

FIGURE 21: AXISYMMETRIC MODES, ANTISYMMETRIC

$K = 0.0001$

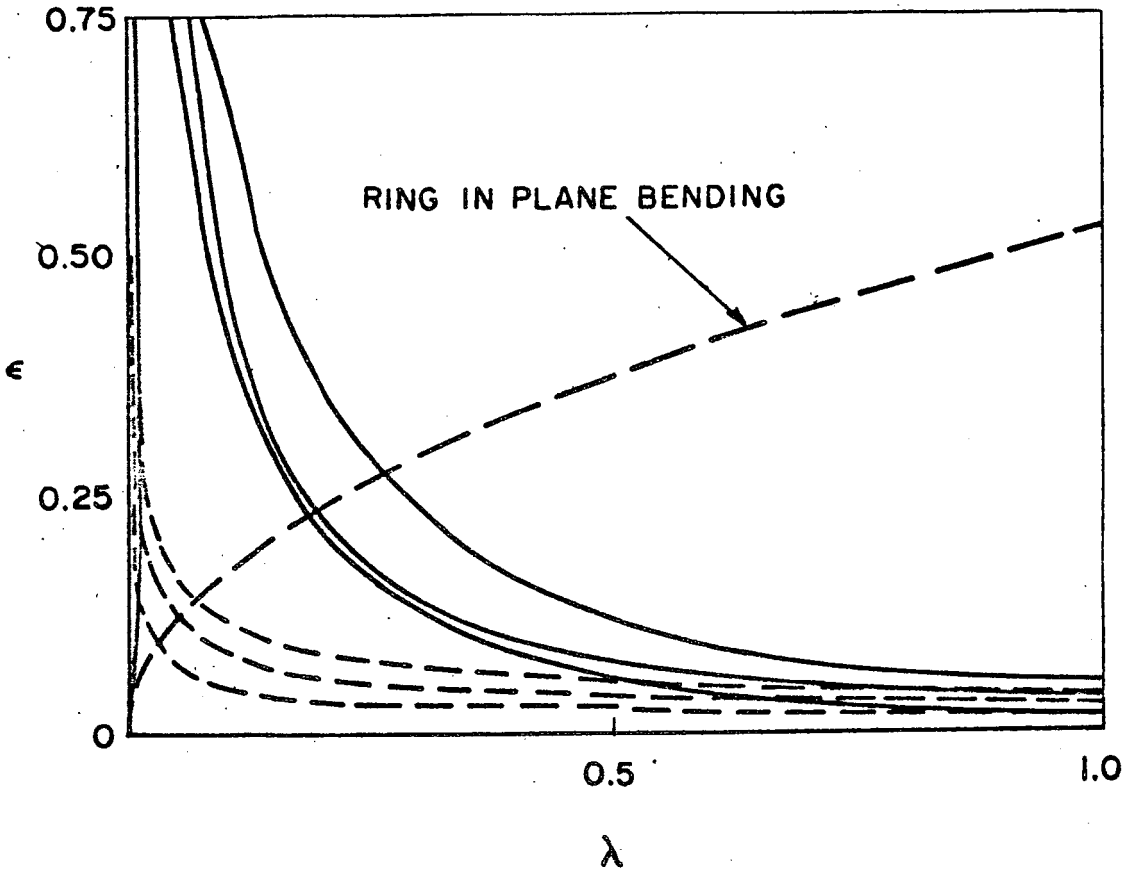

FIGURE 22: n = 2 MODES, SYMMETRIC, κ = 0.0001

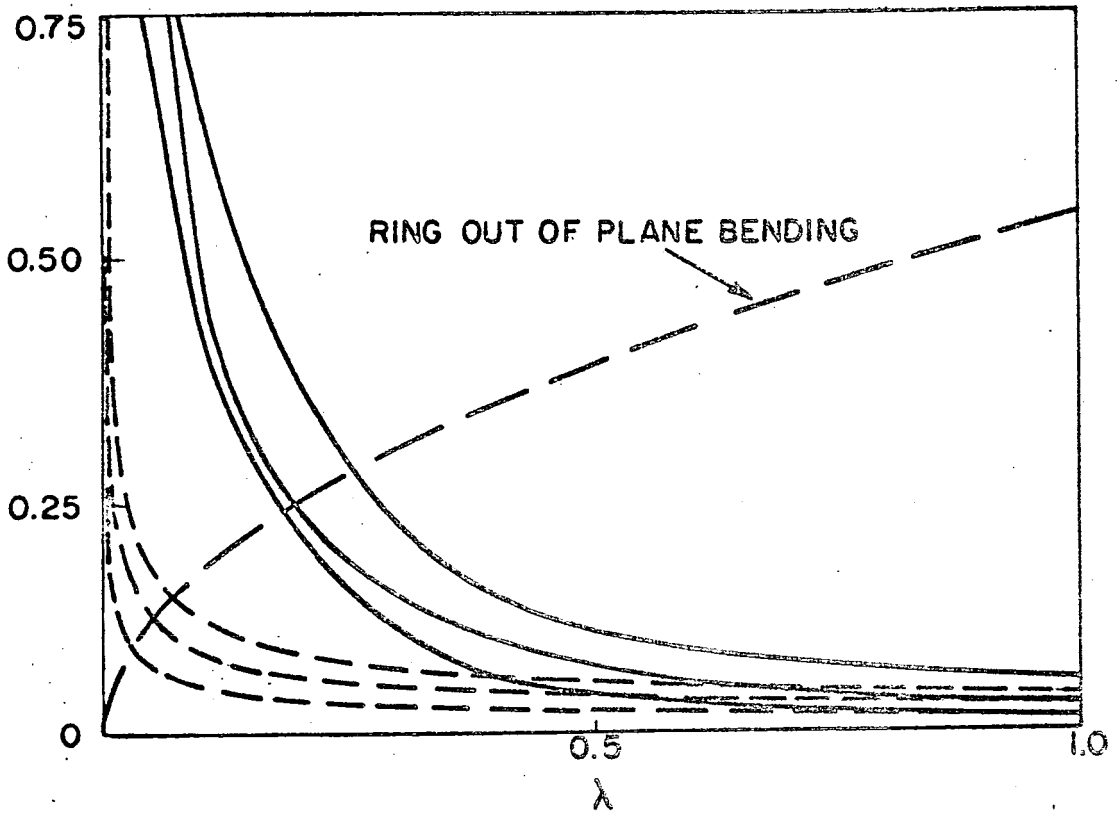

FIGURE 23: n=2 MODES, ANTISYMMETRIC

$\kappa = 0.0001$

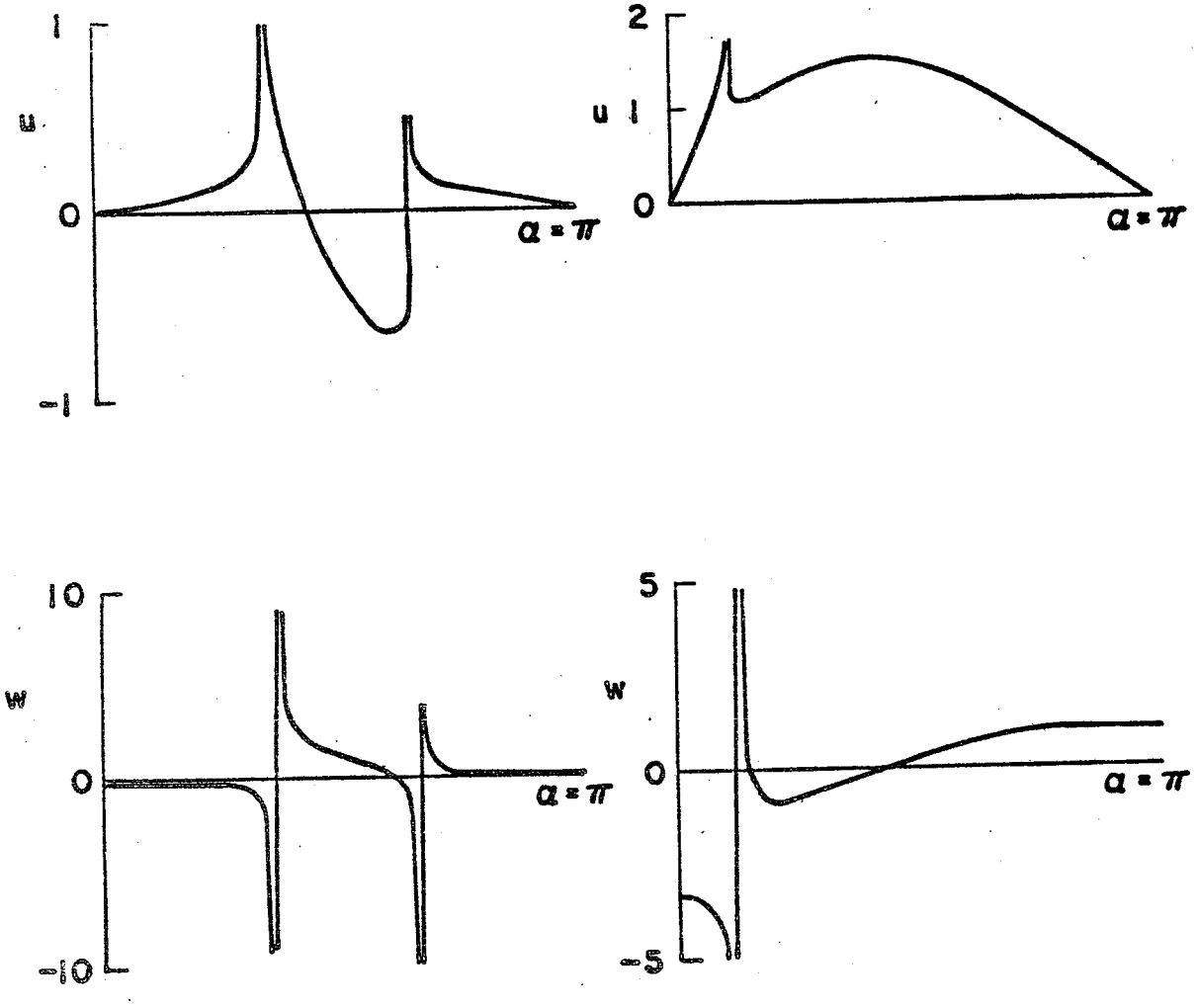

$\epsilon = 0.1$
$\lambda = 0.203$

$\epsilon = 0.1$
$\lambda = 1.04$

FIGURE 24: AXISYMMETRIC MODE SHAPES, SYMMETRIC, K=0

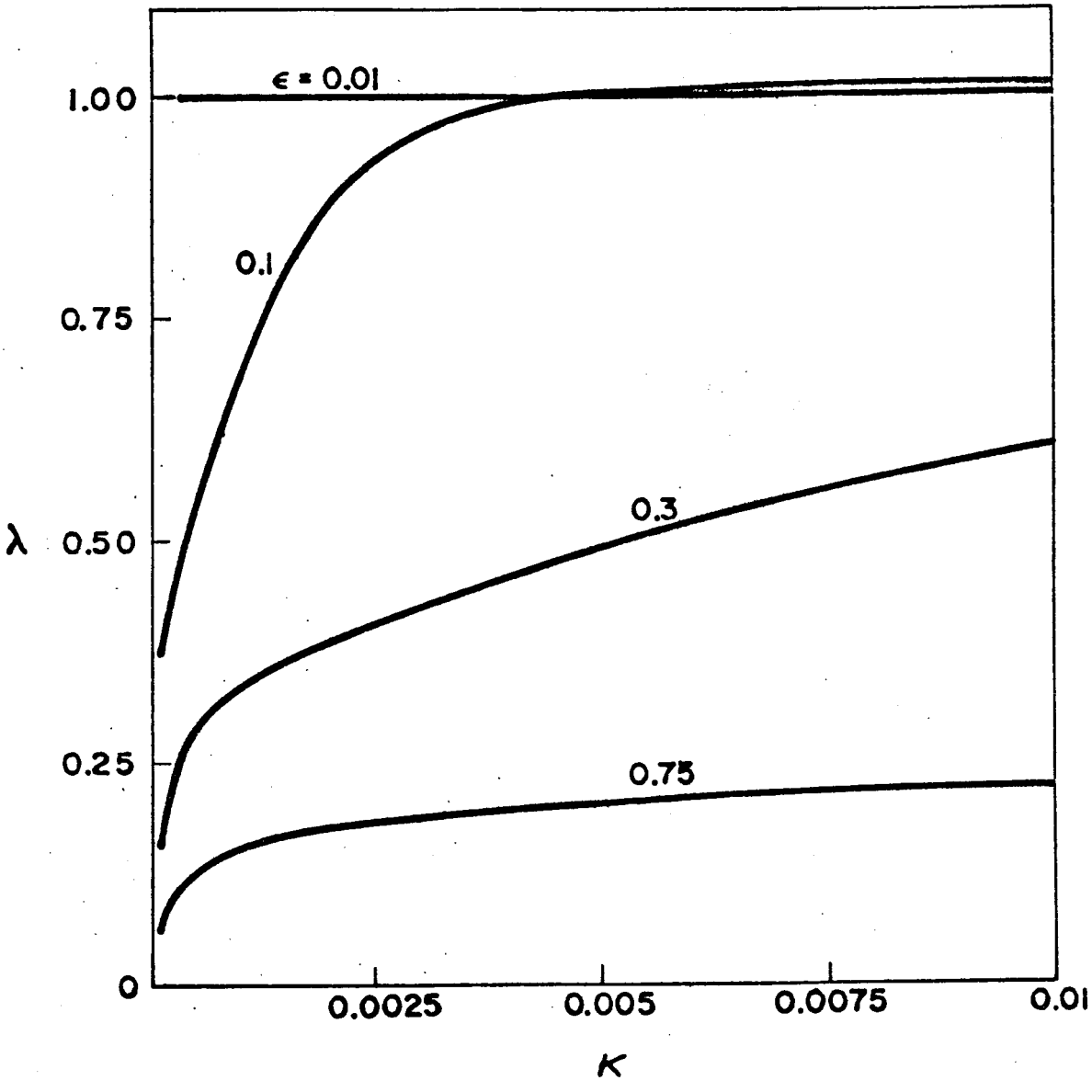

FIGURE 25: FREQUENCY VS PRESTRESS, n = 0,
SYMMETRIC, FIRST MODE

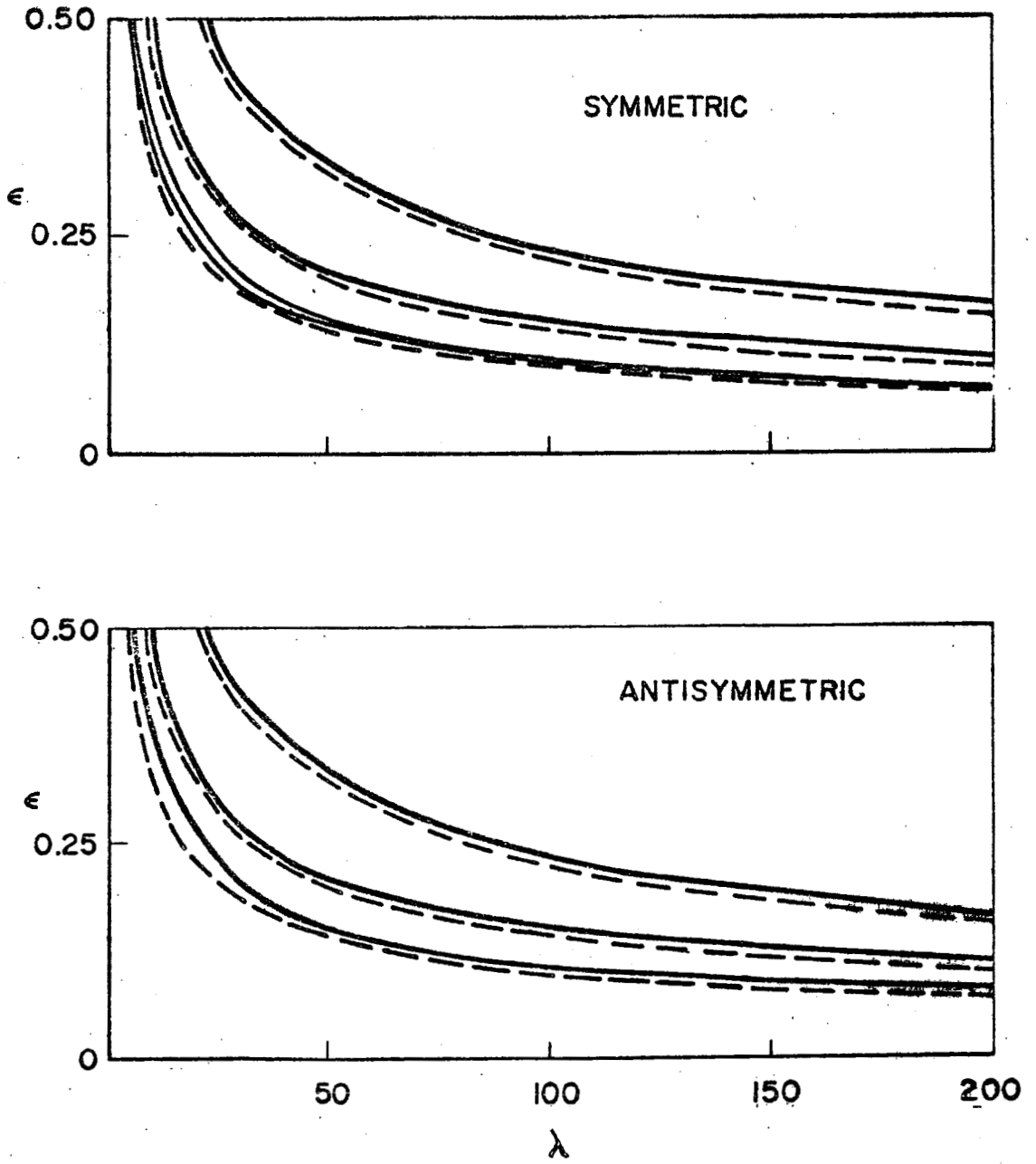

FIGURE 26: UPPER MODE FAMILY, $n = 0, K = 0$

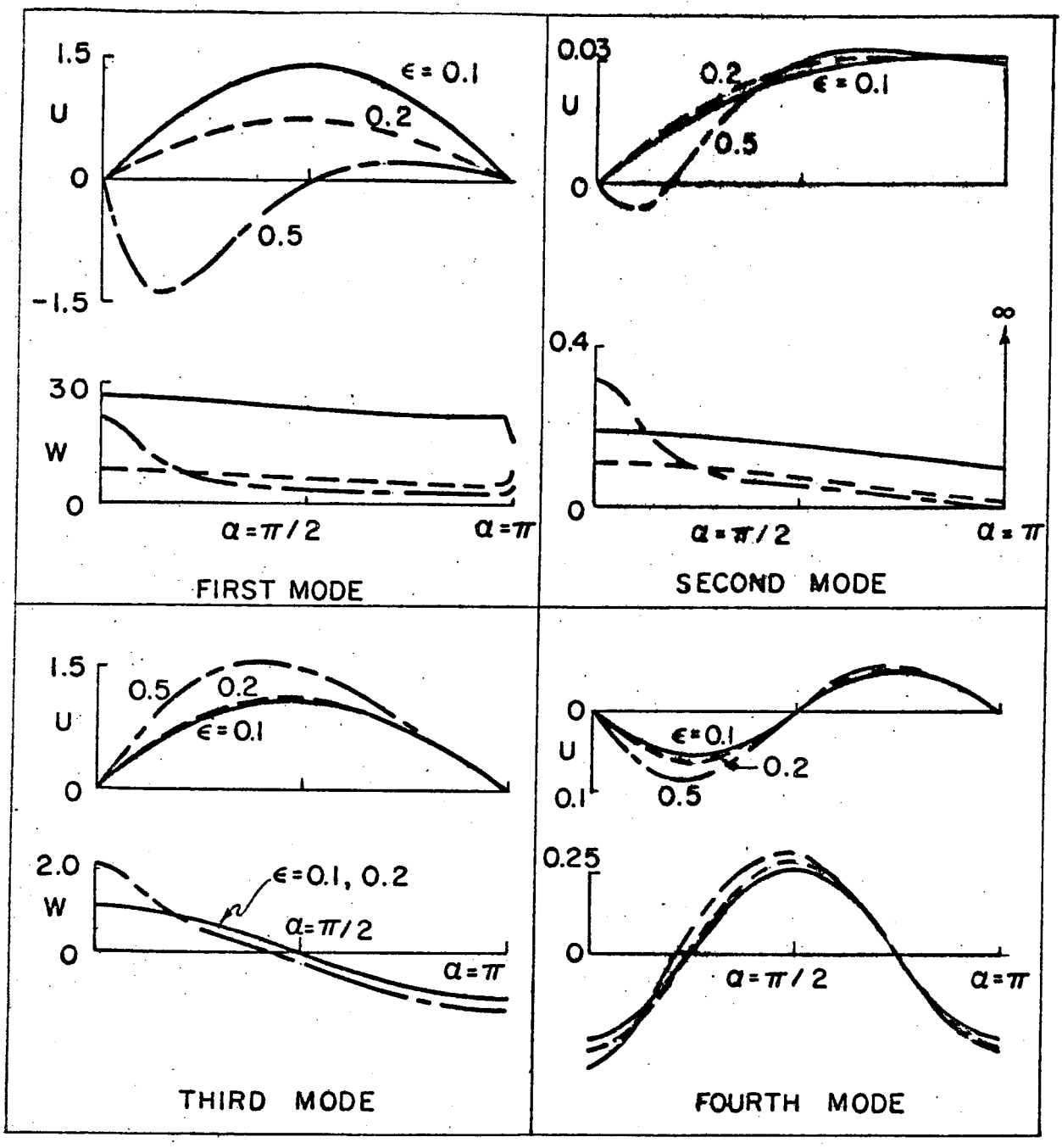

FIGURE 27: UPPER FAMILY MODE SHAPES, SYMMETRIC, $K=0$

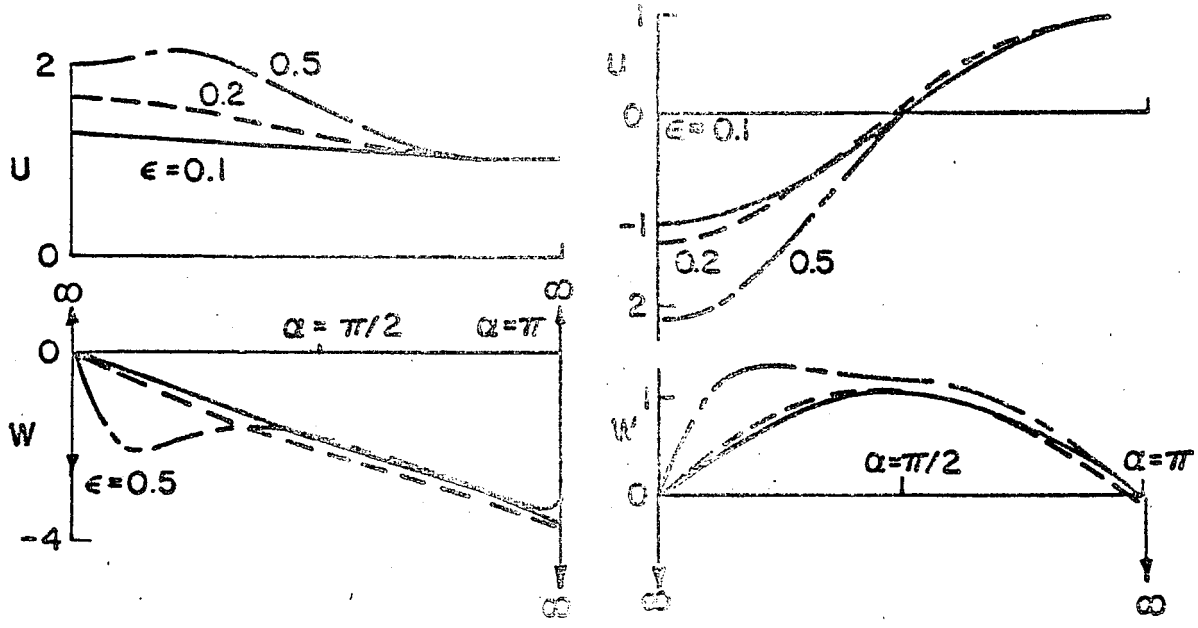

FIRST MODE

SECOND MODE

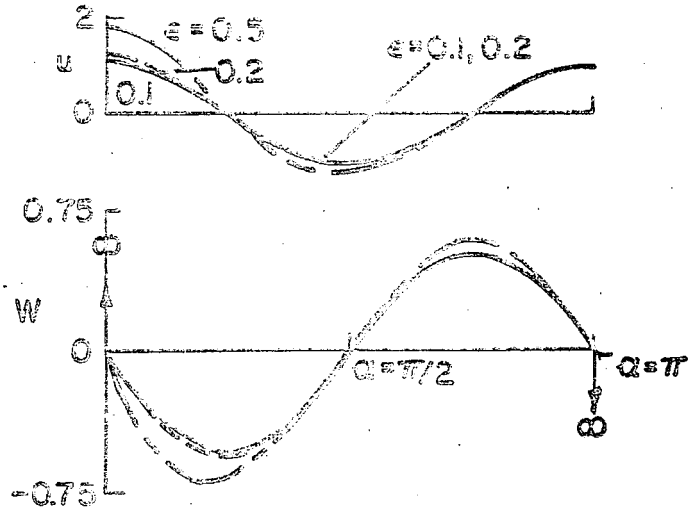

THIRD MODE

FIGURE 28: UPPER FAMILY MODE SHAPES, ANTISYMMETRIC, $\kappa = 0$

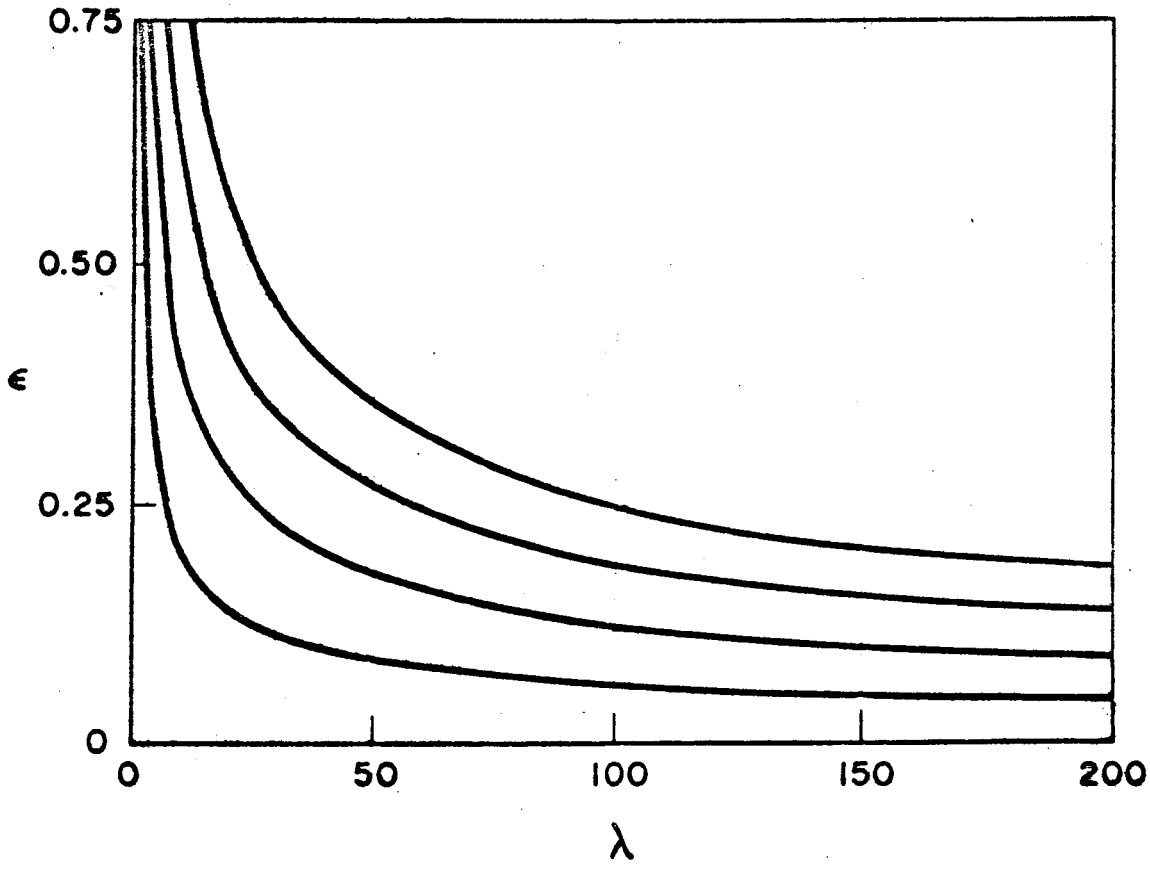

FIGURE 29: CIRCUMFERENTIAL MODES, SYMMETRIC

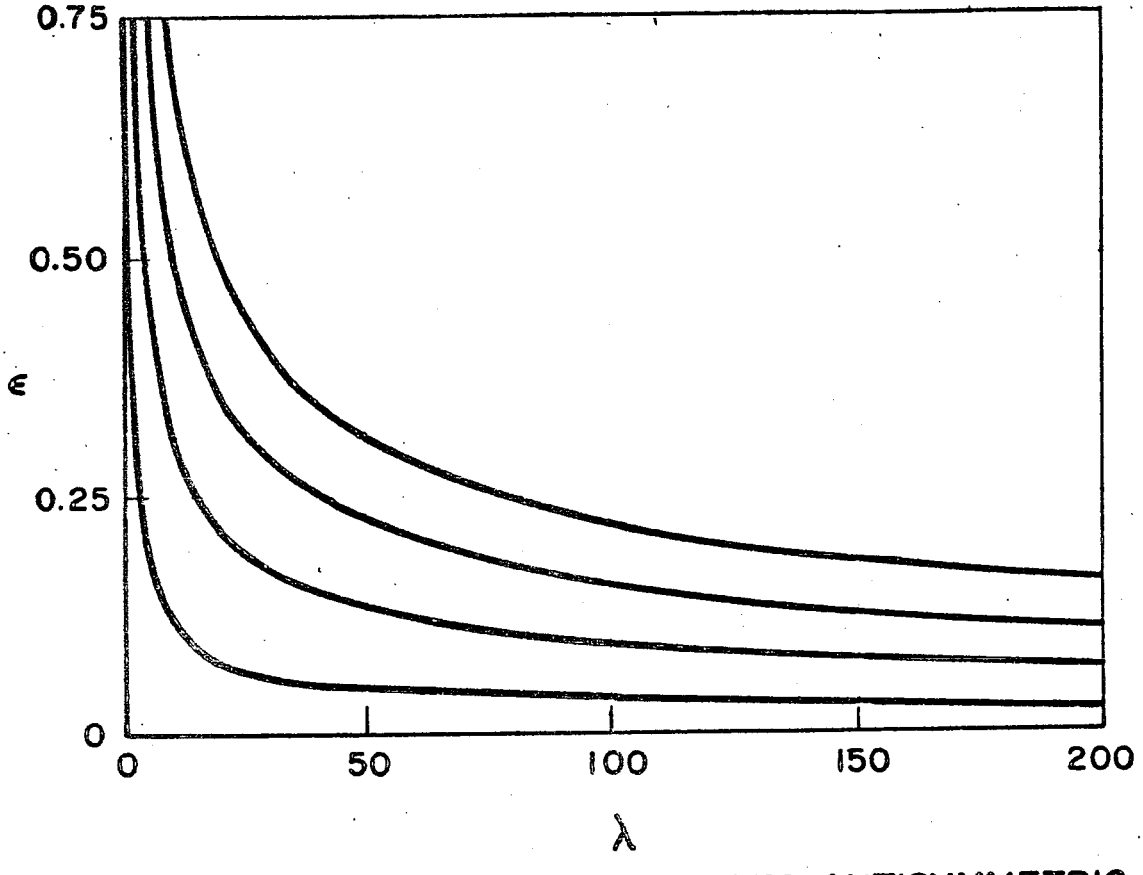

FIGURE 30: CIRCUMFERENTIAL MODES, ANTISYMMETRIC

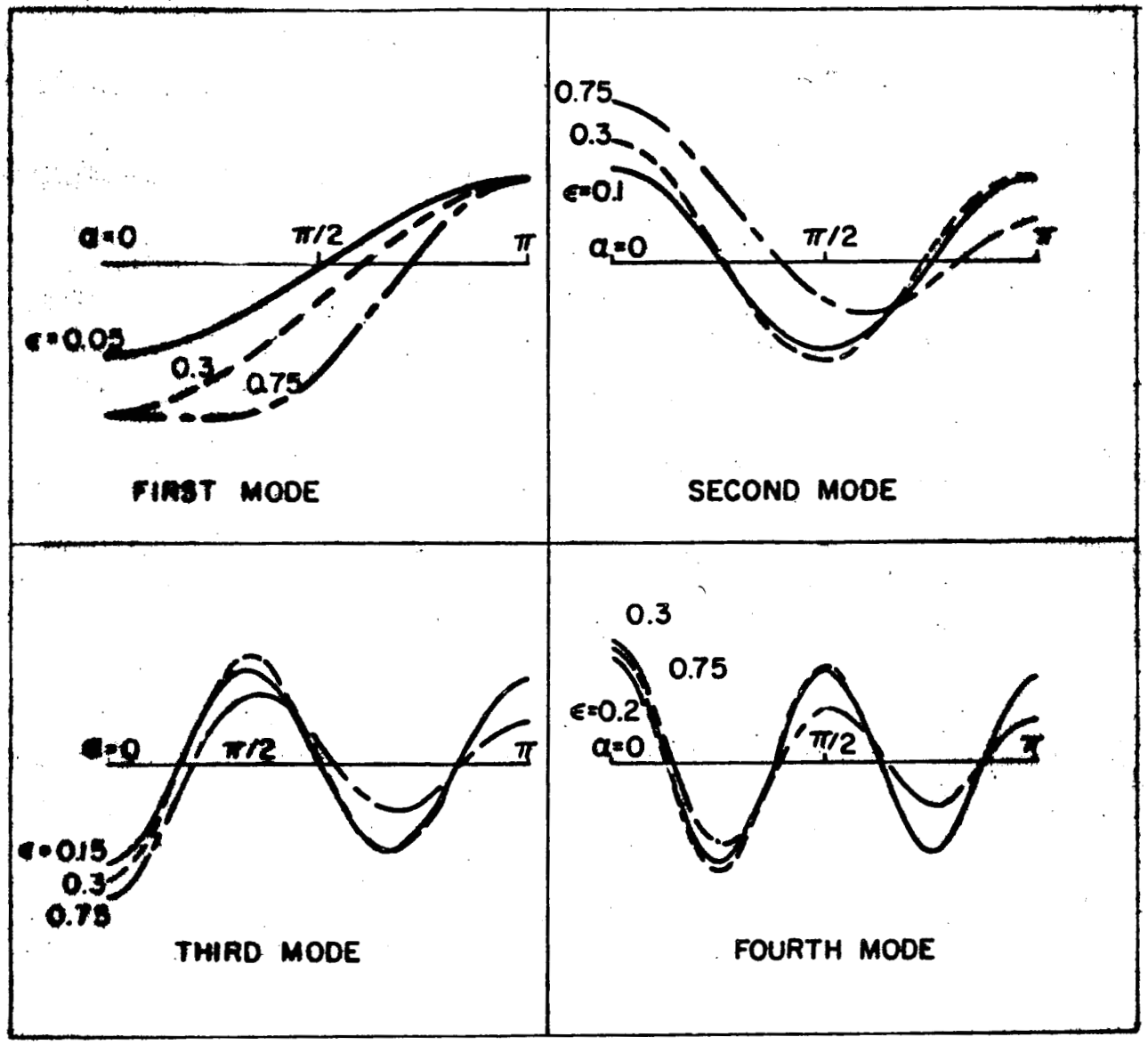

FIGURE 31: CIRCUMFERENTIAL MODE SHAPES (V DISPLACEMENT), SYMMETRIC

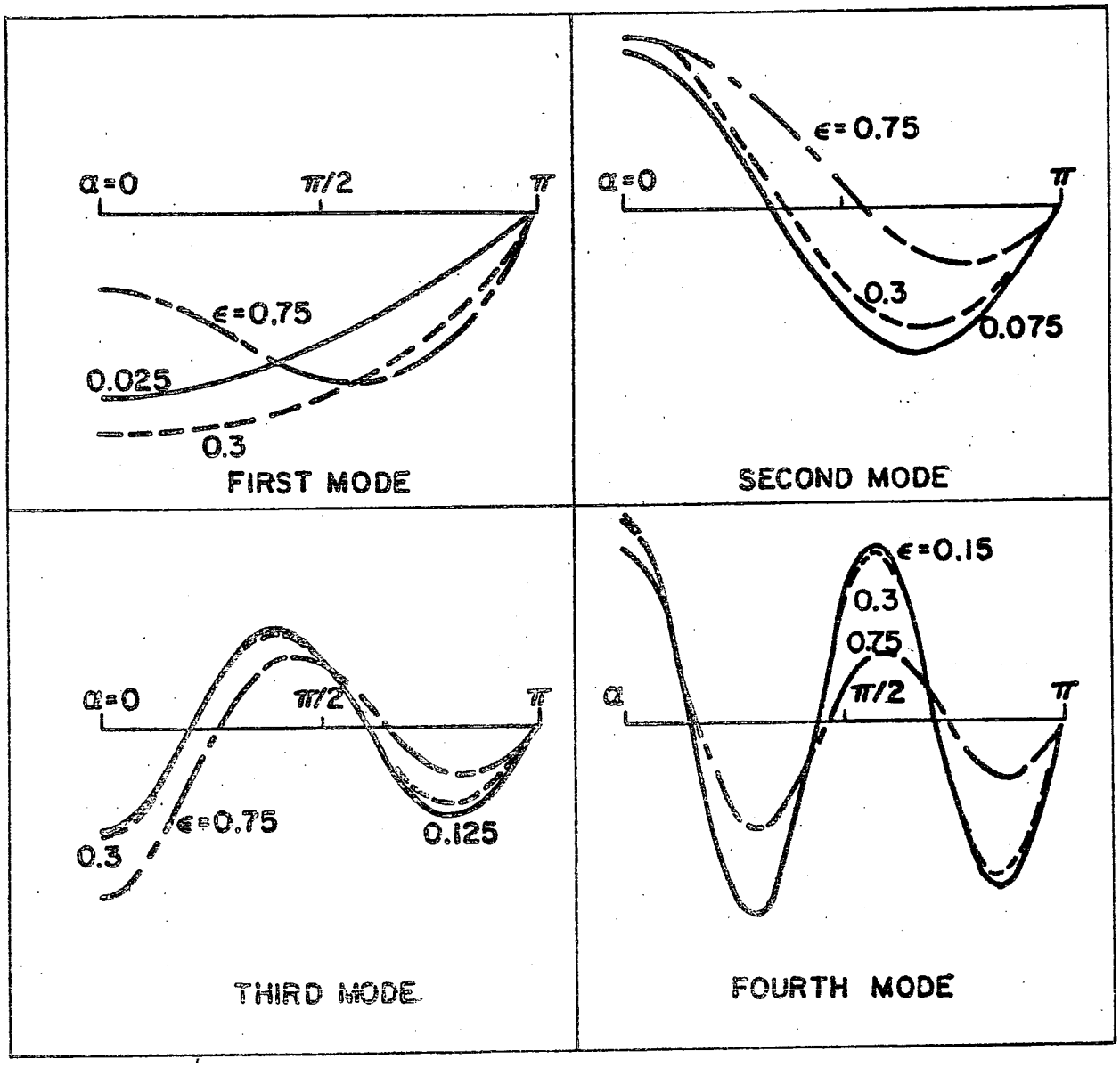

FIGURE 32: CIRCUMFERENTIAL MODE SHAPES (V DISPLACEMENT), ANTISYMMETRIC

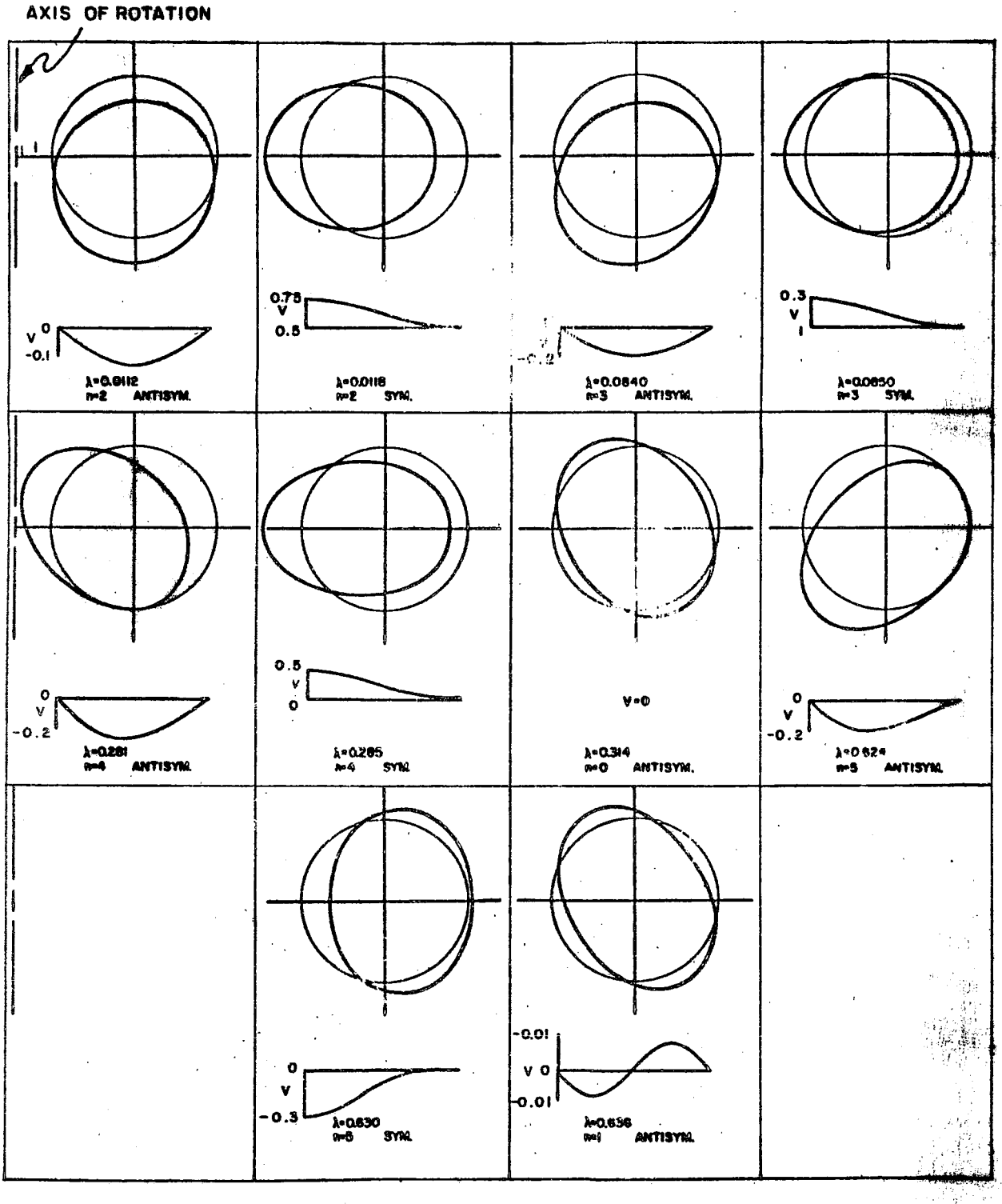

FIGURE 33: CASE I MODE SHAPES

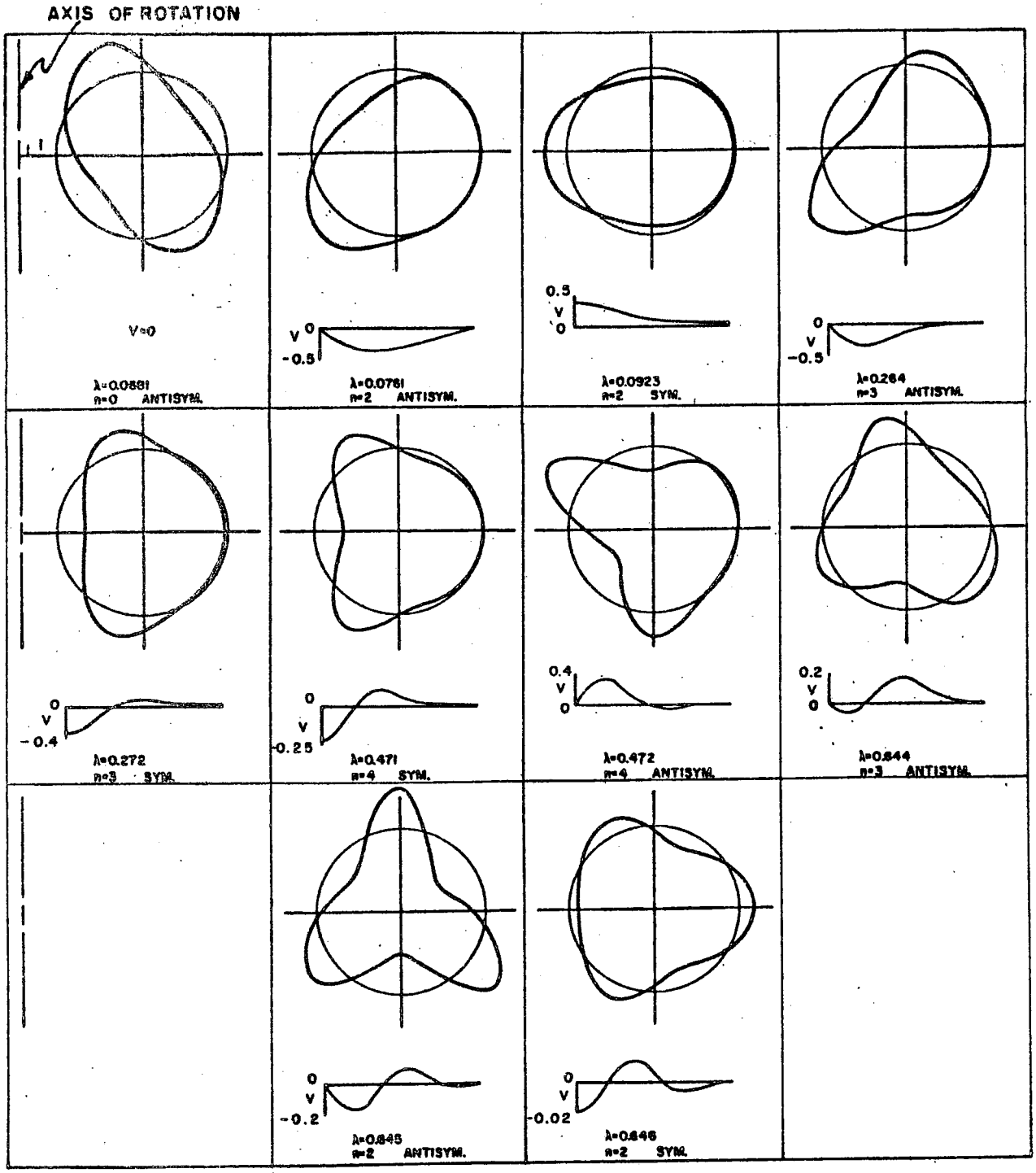

FIGURE 34: CASE II MODE SHAPES